Adrenal rather than hypothalamic-pituitary dysfunction limits HPA axis recovery after chronic glucocorticoid treatment

Lindsey S. Gaston[1], Brenna C. Jorgensen[1], Hannah R. Friedman[1], Marc S. Sherman[2], Joseph A. Majzoub[1]

[1]Division of Endocrinology, Department of Pediatrics, Boston Children's Hospital, Harvard Medical School, Boston, MA, USA

[2]Division of Gastroenterology, Department of Medicine, Massachusetts General Hospital, Harvard Medical School, Boston, MA, USA

*Joseph Majzoub, MD

300 Longwood Avenue, Boston, MA 02115; 617-919-2930

Email: Joseph.Majzoub@childrens.harvard.edu

ORCID ID: 0000-0002-4983-5143

*Lindsey Gaston, MD

300 Longwood, Avenue, Boston, MA 02115; 617-355-7476

Email: Lindsey.Gaston@childrens.harvard.edu

ORCID ID: 0000-0003-3486-7254

Please address reprint requests to Dr. Joseph Majzoub, 300 Longwood Avenue, Boston, MA 02115

This study was supported by NIH 5T32DK007699-39 (LG), NIH F32DK131795-02 (LG), a Pediatric Endocrine Society Research Fellowship Award (LG), a Pediatric Endocrine Society Clinical Scholar Award (LG), a Boston Children's Hospital Office of Faculty Development/Basic & Clinical Translational Research Executive Committees Faculty Career Development Fellowship (LG), and the Thomas Morgan Rotch Harvard Medical School endowment (JAM).

Disclosure summary: The authors have no competing interests to disclose.

Keywords: Glucocorticoids, adrenal suppression, prevention

Abstract

Glucocorticoid-induced adrenal insufficiency (GIAI) can persist for months after discontinuation of chronic corticosteroid therapy, placing patients at risk for life-threatening adrenal crises. This prolonged suppression has been attributed primarily to delayed restoration of hypothalamic–pituitary signaling based on indirect, clinical measures of central axis activity. To identify the rate-limiting site of hypothalamic-pituitary-adrenal (HPA) axis recovery, we systematically evaluated the timing of functional and histologic recovery at each node of the axis following 8 weeks of dexamethasone (DEX) treatment in mice. DEX administration fully suppressed HPA axis activity. Unexpectedly, within one week of DEX withdrawal, hypothalamic *Crh* mRNA and plasma ACTH rebounded above control levels, whereas corticosterone (CORT) remained suppressed for an additional seven weeks. DEX-treated adrenals were markedly atrophic and contained large clusters of lipid-associated macrophages. Even after adjusting for macrophage content, CORT secretion was disproportionately low relative to the remaining adrenocortical cell mass despite supraphysiologic ACTH stimulation. These findings identify the adrenal gland, rather than the hypothalamus or pituitary, as the principal site of persistent dysfunction following glucocorticoid withdrawal. We next tested whether preserving adrenal trophic signaling during glucocorticoid exposure could prevent GIAI. Co-treatment with DEX and daily cosyntropin (a synthetic ACTH analog) failed to preserve adrenal function. In contrast, mice with non-suppressible endogenous ACTH due to targeted deletion of *Nr3c1* (encoding the glucocorticoid receptor) in hypothalamic neurons maintained normal adrenal architecture and steroidogenic capacity despite prolonged DEX treatment. Pharmacologic treatments that mimic sustained, physiologic trophic signaling to the adrenal during chronic glucocorticoid treatment may thus prevent GIAI.

Introduction

Systemic glucocorticoids are prescribed to up to 3% of the population in developed countries for treatment of autoimmune and inflammatory diseases, malignancies, and to prevent allograft rejection[1,2]. Many additional patients are chronically treated with topical and inhaled formulations that can exert systemic effects even at moderate doses[3-5]. Like endogenous cortisol in humans and corticosterone in rodents, exogenous glucocorticoids engage the glucocorticoid receptor (GR) to suppress hypothalamic-pituitary-adrenal (HPA) axis activity through negative feedback. This feedback reduces the synthesis and secretion of corticotropin-releasing hormone (CRH) from the paraventricular nucleus of the hypothalamus and adrenocorticotropic hormone (ACTH) from the anterior pituitary[6]. In the absence of ACTH, a key trophic factor for the adrenal cortex, cortisol-producing cells of the zona fasciculata (zF) undergo both suppression of steroidogenesis and apoptotic cell loss[7,8].

HPA axis suppression is typically transient in patients treated with short-term glucocorticoids. However, treatment exceeding four weeks can cause protracted adrenal insufficiency that can persist for up to a year after steroid withdrawal[9-11]. While awaiting HPA axis recovery, individuals are at risk for adrenal crisis with otherwise routine illnesses or trauma, which has been associated with longer hospitalizations, higher rates of ICU admissions, and even death in patients who are not promptly administered stress-dose steroids[12,13].

Despite the ubiquity of glucocorticoid use and the morbidity of glucocorticoid-induced adrenal insufficiency (GIAI), there are currently no available treatments to prevent or hasten recovery from adrenal suppression. This is due, in part, to the prevailing view that prolonged GIAI is mediated by delayed, post-withdrawal recovery of the hypothalamus and pituitary, which are relatively inaccessible therapeutic targets. Post-withdrawal central suppression was first described by Graber et al., who reported that ACTH levels were inappropriately low to normal for at least two months in patients withdrawn from chronic glucocorticoids despite release from

negative feedback[14]. Since direct ACTH assays had not yet been developed, systemic ACTH levels in this study were interpolated from the corticosterone responses of hypophysectomized rats injected with extracted patient plasma[14,15]. Another study cited inadequate ACTH responses to CRH stimulation testing in patients withdrawn from long-term prednisone as evidence of post-withdrawal central suppression. However, testing was conducted only 24 hours, or two biological half-lives, from the last prednisone dose, thus confounding glucocorticoid-mediated negative feedback and post-withdrawal suppression[16,17]. Post-withdrawal central suppression has also been described after surgical cure of Cushing's syndrome, a state of endogenous glucocorticoid excess, though clinical studies have disagreed as to whether this is mediated by persistent hypothalamic or pituitary dysfunction[18-20].

Interestingly, patients with congenital adrenal hyperplasia, who also require chronic, suppressive glucocorticoid therapy, exhibit elevated levels of ACTH at their morning hydrocortisone trough[21,22]. This suggests that some patients have rapid normalization of hypothalamic-pituitary function after release from glucocorticoid feedback inhibition. The mammalian HPA axis is highly conserved evolutionarily, and all rodent studies have reported rapid restoration of hypothalamic-pituitary function after glucocorticoid treatment. Basal and stimulated ACTH levels (following lipopolysaccharide, arecoline, and CRH administration) were recovered within days of discontinuing 5 or 7 days of methylprednisolone or dexamethasone, respectively, in rats[23,24]. In mice treated with dexamethasone for 30 days, plasma ACTH and corticotrope *Pomc* mRNA levels were elevated above control levels by 1-week post-withdrawal[25]. In all studies, corticosterone (CORT) levels and/or steroidogenic pathway gene expression remained low 5-7 days after discontinuing steroids despite normalization of adrenal

weights[23-25]. Importantly, no animal studies to date have examined HPA axis recovery after longer courses of glucocorticoids known to cause protracted adrenal suppression in humans.

Given these discrepancies in the existing clinical and preclinical literature, we developed a murine model of GIAI to define the locus and mechanisms underlying persistent HPA axis dysfunction following withdrawal of long-term glucocorticoid treatment. After we discovered that adrenal dysfunction persists for months after steroid withdrawal despite rapid restoration of hypothalamic-pituitary signaling, we tested whether preserving adrenal trophic signaling during glucocorticoid exposure, using either a pharmacologic or genetic approach, could prevent GIAI.

Materials and Methods

Animals

All animal protocols were in accordance with the National Institutes of Health guidelines and were approved by the Animal Care and Use Committee of Boston Children's Hospital (Protocol 00001983). Mice were housed on a 12-hour/12-hour light-dark cycle (lights on at 7 am) with ad libitum access to rodent chow and water unless otherwise indicated. Mice used for studies were all aged either 8 weeks at the time of DEX initiation (long-term studies) or 8-16 weeks (DEX-naïve controls or short-term studies).

Wild-type (WT) mice: C57BL/6J mice (The Jackson Laboratory, Bar Harbor, ME) were maintained by breeding within our population.

Sim1^{Cre}:GR$^{fl/fl}$ mice (HGRKO): Sim1^{Cre} mice (generous gift of Brad Lowell, Beth Israel Lahey Medical Center, Boston, MA) were bred to floxed GR exon 3 mice (B6.Cg-*Nr3c1$^{tm1.1Jda}$*/J, Catalog #021021, The Jackson Laboratory, Bar Harbor, ME), both maintained on an inbred C57BL/6J background[26,27]. Littermates that were Cre negative but had GR exon 3 floxed alleles

were used as controls. Genotyping was performed using the primers and conditions detailed in Table SI.

Pharmacologic treatments: Mice were treated with either water-soluble dexamethasone (Sigma-Aldrich 2915) at a concentration of 3.6 mcg/mL (~20 mcg/day assuming an average water intake of 5.8 mL/day[28]) or no-drug control via drinking water for either 4 days (short-term) or 8 weeks (long-term studies). When specified, mice were co-treated with 10 mcg/kg cosyntropin, (synthetic ACTH[1-24], Sandoz, NDC 0781-3440-95), dissolved at 10 mcg/mL in 0.9% saline. Cosyntropin was administered once daily by intraperitoneal injection at 16:30 to align with the murine circadian ACTH peak for either 4 days or 8 weeks, as above.

Hormonal assays: All testing was performed, as specified, on separate days so that no mouse was bled more than once on a given day. Plasma for measurement of corticosterone and ACTH was obtained by rapid retroorbital phlebotomy without anesthesia into EDTA-coated capillary tubes with a total time from first handling the animal to completion of bleeding not exceeding 30 seconds. Basal/unstimulated phlebotomy was performed at 16:30 in a ventilated hood in the same room in which the animals were housed. Cosyntropin stimulation[29], insulin-induced hypoglycemia testing (1 U/kg dose)[30], and physical restraint (20 minutes)[30] were all performed as previously published. Blood was collected on ice, and plasma was separated by centrifugation at 1500 RPM at 4°C and stored at -80°C until assay. Plasma concentrations of corticosterone (ALPCO, 55-CORMS-E01) and ACTH (ALPCO, 21-ACTHU-E01) were measured by ELISA per manufacturer instructions. For the ACTH assay, plasma was diluted 1:10 with ACTH 0 calibrator (ALPCO; 11-C-270-10-G25). The lower limit of detection is 0.061 mcg/dL and 0.22 pg/mL for the CORT and ACTH assays, respectively.

Necroscopy and tissue preparation: Animals were euthanized by rapid decapitation without anesthesia followed by necroscopy for isolation of hypothalami and adrenals. Thick coronal sections flanking the hypothalamus were prepared with a surgical blade and then fixed

in 10% formalin overnight before transfer to 70% ethanol while awaiting paraffin embedding. Adrenals were trimmed of surrounding fat tissue, rinsed in phosphate-buffered saline (PBS), and weighed before overnight fixation in 10% neutral buffered formalin.

Single-molecule RNA in situ hybridization

Three 5 µm-thick coronal brain sections were mounted onto each slide, and every other slide was stained with hematoxylin and visualized with brightfield microscopy (Nikon E800). The paraventricular nucleus was identified histologically based on its characteristic “butterfly-shaped” appearance in coronal sections, which was used to anchor selection of 2 unstained slides immediately rostral and caudal to this structure for analysis. Single-molecule RNA in situ hybridization was performed using a catalog Mus musculus *Crh* probe (ACD #316091) and 2.5 HD RED detection kit (ACD #316091) following manufacturer’s protocol. Slides were counter stained with 50% Gill’s Hematoxylin II and mounted with EcoMount. Positive control *Ppib (*ACD #313911) and negative control *dapB (*ACD #310043) were used in every experiment to ensure sample quality. Brightfield images at 40x magnification were generated with an Olympus VS120 Virtual Slide Scanner and then analyzed with semi-quantitative densitometry using the Weka Segmentation plugin for Fiji ImageJ per ACDBio instructions[14]. Analysis was restricted to freehand sections encompassing the characteristic “butterfly” morphology of PVH cell bodies. CRH expression, reported as arbitrary units (AU), was quantified by dividing the area of the *Crh* densitometric signal (μm^2) by the total area of this region (mm^2).

Total mRNA and protein staining

To quantify total mRNA *in situ*, FFPE sections were deparaffinized and antigen-retrieved in buffer TE (pH=9). We then adapted the protocol in Farny *et al.* and Hurt *et al.* to label polyA-

capped RNAs on FFPE sections using Cy5-conjugated polyDT (26-4430-02, GeneLink)[31,32]. Total protein *in situ* was measured using the N-Hydroxysuccinimide (NHS) ester method; NHS esters react with primary amines and well-approximate total protein mass[33,34]. Briefly, FFPE sections were deparaffinized and antigen-retrieved in buffer TE (pH=9). Slides were stained with NHS-Alexa 568 dye conjugates (Thermo Scientific A20003) in PBS for 30 minutes and then washed 5X in PBS.

Paraffin section immunofluorescence

After fixation, adrenals were oriented with their broadest surface parallel to the cutting plane in 4% low-melting-temperature SeaPlaque agarose (Lonza, #50101). Agarose blocks were then dehydrated in ethanol, xylene, and embedded in paraffin blocks. Paraffin sections were cut at 5 µm thickness, and immunofluorescence was performed as described in Leng *et al.*[35] with the antigen retrieval conditions and antibody concentrations detailed in Table SII. When indicated, Streptavidin, Alexa Fluor 488 Conjugate (Invitrogen, #S112233) was added to the secondary antibody solution at a final concentration of 1:500. In all experiments, sections were incubated in TrueBlack Lipofuscin Autofluorescence Quencher (Biotium, #23007) in 70% ethanol at room temperature for 3 minutes and rinsed three times in PBS prior to mounting with Prolong Gold Antifade Mountant with DAPI (Invitrogen, #P36931). Images were acquired with either a Nikon upright Eclipse 90i microscope with a 20x/0.75 Plan-Apochromat objective or an Olympus VS120 Virtual Slide Microscope using a 20x objective and adjusted for brightness and contrast in ImageJ.

Floating section immunofluorescence.

After fixation, adrenals were oriented with their broadest surface parallel to the cutting plane in 4% low-melting-temperature SeaPlaque agarose (Lonza, #50101) and sectioned at a thickness of 100 µm with a vibratome. Individual slices were separated by free floating in PBS. Sections were wet mounted in PBS on Superfrost Plus slides (Fisher Scientific, 12-550-15) and imaged with a 4x objective on a Nikon E800 brightfield microscope. The area of each section was measured in ImageJ, and the largest section was selected for subsequent immunostaining. Floating section immunofluorescence was then performed as per Leng *et al*[35] with the addition of Streptavidin, Alexa Fluor 488 Conjugate (1:500, Invitrogen, #S112233) to the secondary antibody solution. Images were acquired with a Nikon Ti2 microscope with a Yokogawa CSUW1 confocal unit, a Nikon Plan Apo Lambda 20x objective lens and a Zyla 4.2 PLUS sCMOS camera (ANDOR). All images were taken with identical laser strength, gain and exposure settings for the 405nm (used to capture autofluorescence), 488nm, and 647nm channels. Each image was acquired using the Large Image function in the NIS elements software. This function allowed us to take images in a 4x4 grid with 15% overlap, allowing the images to be stitched together. Brightness and contrast were adjusted in ImageJ.

Image analysis

Fluorescent images were analyzed using QuPath (version 0.4.3), an open-source software for digital pathology.

Positive Cell Detection: QuPath's cell detection feature was employed to label cells as either Ki-67 or TUNEL positive based on co-localization of the 647 nm channel signal with the DAPI nuclear signal. Images were opened in fluorescence mode, and regions of interest (ROI) were manually defined to include only the adrenal cortex based on morphologic characteristics. ROI were further restricted to the zF for Ki-67 analysis, as defined by DAB2-negative cortical cells. The "cell detection" feature was then run specifying DAPI as the detection channel and the

647 nm channel nuclear (Ki-67 analysis) or cellular (TUNEL analysis) mean as the score compartment. Nuclear size and intensity threshold parameters for both were adjusted and inspected visually to ensure accurate positive cell detection. Any cell exhibiting signal overlap between the DAPI and 647 nm channels above the specified thresholds was classified as either TUNEL or Ki-67 positive and reported as a percentage among total cells.

Morphometry: Morphometric analysis was performed on thick, floating section immunofluorescent specimens to quantify the area of either the adrenal cortex (Streptavidin staining, 488 nm channel), medulla (tyrosine hydroxylase immunostaining, 647 nm channel), or adrenal macrophages (autofluorescence, 408 nm channel) based on signal intensity across multiple channels using the “create thresholder” function in QuPath. Images were opened in fluorescence mode, and brightness/contrast of individual channels were adjusted for optimal signal visualization. ROI were manually defined to include the entire adrenal slice but not surrounding adipose tissue. For each channel, QuPath’s intensity thresholding was applied to ensure accurate delineation of stained or autofluorescent areas, as confirmed by visual inspection. As DEX treatment has been shown to attenuate streptavidin staining in the murine zF, we applied a lower threshold in 8+0 adrenals to ensure detection of all residual adrenocortical tissue[36]. The area of tissue with a signal above this threshold for each channel was classified as positive and reported in square microns.

Statistics

Two-tailed Student’s t tests were performed to compare significance between two groups. Comparisons done beyond 2 groups were performed by ANOVA, and Bonferroni correction was applied for post-hoc, pairwise multiple comparison testing. Nonlinear regression using an exponential growth equation was used to model stimulated CORT recovery (dependent variable) over time (independent variable), and doubling time was computed as ln(2)/K where K

is the rate constant. When two exponential growth models were compared, the extra-sum-of-squares test was employed to determine whether the exponential equations provided significantly different fits to the data. All statistical analyses were performed in GraphPad Prism v.10.3.1. Windows, GraphPad Software, Boston, Massachusetts USA, www.graphpad.com. *P* values below 0.05 were considered statistically significant.

Study approval

All animal experiments were approved by the Boston Children's Hospital Institutional Animal Care and Use Committee (Protocol Number 00001983).

Results

Mice treated with long-term dexamethasone (DEX) have protracted adrenal insufficiency despite early hypothalamic-pituitary recovery

We first established when hormonal function recovered at each node of the HPA axis following long-term DEX treatment. Adult, male, WT mice were treated with either continuous DEX or vehicle (DEX-naïve, or DN) in the drinking water for 8 weeks. Starting at the time of DEX withdrawal (8+0) and at 1-2 week intervals through 8+8 (where A weeks of treatment plus B weeks of withdrawal = A+B), separate cohorts of mice underwent serial cosyntropin stimulation and insulin-induced hypoglycemia (IIH) testing followed by necroscopy (Model 1, Fig. S1)

As expected, long-term DEX treatment suppressed *Crh* mRNA within the paraventricular nucleus of the hypothalamus (PVH; 28±5 in 8+0 vs. 156±32 arbitrary units [AU] in DEX-naïve (DN) control animals, $p<0.05$). However, *Crh* expression recovered to control levels 1 week after DEX was discontinued (8+1; 159±28 AU vs. DN, $p=0.96$; Fig. 1*A, B*). Similarly, IIH-stimulated plasma ACTH concentrations were suppressed during the period of glucocorticoid exposure

(4.2±3.6 pg/mL at 8+0) but rebounded significantly above control levels by 1-week post-withdrawal (1707±85 pg/mL at 8+1 vs. 875±44 pg/mL, $p<0.001$). IIH-stimulated ACTH levels remained elevated through 4 weeks post-withdrawal and reached a peak two weeks after completion of DEX treatment (Fig. 1*C*). Despite this, both IIH- and cosyntropin-stimulated CORT levels remained significantly lower than DN controls until 8 weeks after DEX cessation (Fig. 1*D*, *E*). Thus, mice withdrawn from long-term DEX have delayed recovery of CORT secretion despite rapid restoration of hypothalamic-pituitary function.

Long-term DEX induces adrenocortical atrophy with accumulation of large macrophage clusters

Having found the adrenal to be the limiting site of post-withdrawal GIAI, we then assessed adrenal mass and histology at select timepoints after chronic DEX. At 8+0, adrenal mass was reduced by 60% compared to controls (1.0±0.041 mg vs. 2.5±0.063 mg in DN, $p<0.0001$, Fig. 2*A*). Although adrenals from DEX-exposed adrenals weighed significantly less than those from DN controls through 6 weeks post-withdrawal, divergent patterns of recovery were noted for adrenal mass vs. function. Adrenal mass nearly doubled between 0 to 1 weeks post-withdrawal to 75% of controls (1.9±0.11 mg at 8+1) and remained relatively stable over the remaining recovery period. In contrast, CORT secretion was 75% lower than control values at 8+1 and more gradually recovered over the subsequent 7 weeks (Fig. S2*A*, *B*; raw data derived from Figs. 1*D*, *E* and 2*A*)

Hematoxylin and eosin staining revealed that DEX caused striking adrenocortical atrophy followed by gradual re-accumulation of cortical tissue in the 8 weeks post-withdrawal (Fig. 2*B*). Interestingly, DEX-exposed adrenals contained large, vacuolated structures with reduced nuclear density near the corticomedullary junction that persisted through 8 weeks post-withdrawal (Fig. 2*B*, magnification in 2*E*). These clusters were intensely autofluorescent, which was attenuated with the addition of TrueBlack, a lipofuscin autofluorescence quencher[37] (Fig. S3*A*, *B*). ISH with

a 5'-Cy5-Oligod(T)30 demonstrated similar nuclear mRNA poly(A) content in these structures compared to surrounding cortical cells (Fig. S3*C*)[31,32]. The large, vacuolated, extranuclear space in these clusters was not strongly labeled with 568 NHS Ester (SE), a total protein stain (Fig. S3*D*)[33,34]. Together, this suggests that the multinucleated clusters observed in DEX-exposed adrenals contain live, lipofuscin-rich, biologically active cells rather than acellular, proteinaceous debris. These cells were negative for the steroidogenic enzyme *Cyp11b1* mRNA, a marker of zona fasciculata (zF) cells (Fig. S3*E*).

Immunostaining with the myeloid-specific marker, CD68, and macrophage-specific marker, F4/80, identified these cells as clusters of adrenal macrophages (AMs). Rare, mononuclear CD68- and F4/80-positive cells were visualized in the adrenal cortex (labeled with fluorescent 488-conjugated streptavidin[36]) of DN mice (Fig. 2*C*, *D*). Increased CD68- and F4/80-positive macrophages were present in the adrenal cortex after 2 weeks of DEX treatment (2+0). After 8 weeks of DEX (8+0), large AM clusters accumulated at the corticomedullary junction (Fig. 2*C*, *D*, magnified in 2*F*, *G*) and appeared to fragment and migrate into the adrenal medulla by 8 weeks post-withdrawal (8+8). AMs contained lipid, detected by both oil red O and BODIPY staining, but were negative for the lipid droplet associated proteins perilipin-1 and 2 (PLIN 1 and 2; Fig. S4*A*-*D*). AMs were also positive for CD11c and *Trem2* by IF and ISH, respectively, both of which are expressed by lipid-associated macrophages in the context of metabolic-associated steatohepatitis and atherosclerosis (Fig. S4*E, F*)[38-41].

CORT secretion is disproportionately low relative to steroidogenic cell mass for at least 2 weeks post-DEX

As AMs likely contribute to adrenal mass but not biosynthetic function, we then asked specifically how the steroidogenic cell population contracted and recovered after chronic DEX treatment. To do this, we performed morphometric analysis on thick, immunostained adrenal

sections, from which we selected the largest, equatorial one from each gland. Steroidogenic adrenocortical cells were labeled with 488-streptavidin[36] (green), and the medulla was identified by immunofluorescence for tyrosine hydroxylase (red). Sections were not treated with TrueBlack so that AMs could be identified by endogenous autofluorescence (cyan; Fig. 3*A*).

As observed with adrenal weights (Fig. 2*A*), pan-cortical area, which includes both streptavidin-positive and autofluorescent regions, decreased with DEX treatment (764±284 mm^2 in 8+0 vs. 1596±319.4 mm^2 in DN) but nearly normalized by 1-week post-withdrawal (1100±72 mm^2 in 8+1, Fig. 3*A*, *B*). Medullary (TH-positive) area was comparable at all time points, indicating that relatively equivalent, equatorial adrenal sections were used for morphometric analyses ($p=0.15$, Fig. 3*C*). Autofluorescent AM area increased with DEX treatment and remained stably elevated through 8 weeks post-withdrawal (Fig. 3*A*, *D*). Steroidogenic cell type area, computed by subtracting AMs (cyan autofluorescence) from the pan-cortical (green) area, markedly decreased with DEX treatment (272±47 mm^2 in 8+0 vs. 1286±153 mm^2 in DN, $p<0.001$) but more than tripled in the first week post-withdrawal (887±70mm^2; Fig. 3*A*, *E*).

To examine how adrenal function relates to adrenocortical cell mass, we calculated the ratio of cosyntropin-stimulated CORT secretion to the steroidogenic cell type area, normalized to DN controls (Fig. 3*F*). This ratio decreased at the end of DEX treatment (0.60±0.14, $p=0.05$) but reached its lowest values at 1- and 2-weeks post-DEX (0.58±0.05 and 0.44±0.05, $p<0.05$ vs. DN). By 8+6, the ratio had returned to baseline (0.99±0.01) and was elevated relative to DN by 8+8 (2.0±0.18, $p<0.001$ vs DN). These findings indicate that, for at least 2 weeks after DEX withdrawal, CORT secretion is disproportionately low compared to the size of the non-macrophage adrenal cortex, even under supraphysiologic ACTH stimulation.

Immunofluorescence for CD31 revealed preserved vascularity in both DEX-treated (8+0) and withdrawn (8+1) adrenals (Fig. S5*A*). The zona glomerulosa, labeled by Dab2, thickened during chronic DEX exposure (45±2.6 µm at 8+0 vs. 36 ± 0.96 µm in DN) but returned to baseline by

8+1 (36±2.2 µm; Fig. S5B and C). Ki-67 staining demonstrated a robust increase in adrenocortical proliferation within one week of DEX withdrawal (17±1.5% of 8+1 cells vs. 2.0 ± 1.0% of DN cells; Fig. S5B and D), consistent with the known mitogenic effects of ACTH[42]. Together, these findings indicate that disproportionately low CORT secretion relative to steroidogenic cell type area cannot be explained by impaired adrenal vascularity, zonation, or trophic signaling but instead reflects a selective defect in CORT biosynthesis or secretion.

Maintenance of endogenous ACTH secretion but not intermittent cosyntropin administration during the period of DEX exposures prevents GIAI

Having localized post-withdrawal GIAI to the adrenal, we next tested whether maintaining trophic stimulation during glucocorticoid exposure could prevent adrenal suppression. Wild-type mice were treated with DEX as above and received daily, intraperitoneal injections of cosyntropin (ACTH[1-24]; DEX+COS) for either 4 days (short-term) or 8 weeks (long-term). Long-term cohorts underwent either a) serial cosyntropin stimulation testing at 1–2-week intervals from 0-8 weeks after withdrawal, or b) necroscopy at 8+1 (Model 2, Fig. S1). Short-term DEX+COS treatment significantly but variably reduced DEX-induced adrenocortical apoptosis (5.7±1.7% vs. 11±0.8% in 4D DEX glands; Fig. 4*A*, *B*). In contrast, after 8 weeks of treatment (8+0), cosyntropin-stimulated CORT levels remained equally suppressed in DEX+COS and DEX-only mice (2.0±1.0 µg/dL vs. 2.0±0.61 µg/dL, p=0.99). Following withdrawal, CORT recovery was significantly delayed in DEX+COS mice (doubling time=5.2 weeks) compared to DEX-only mice (2.5 weeks; p=0.0009, Fig. 4*C*). Morphometric analysis at 8+1 revealed comparable steroidogenic cell type area between DEX+COS and DEX-only adrenals (Fig. 4*D*, *G*) but reduced AM area in the DEX+COS group (Fig. 4*F*). AM morphology was also heterogeneous, ranging from scattered smaller cells throughout the zona fasciculata to typical aggregates at the corticomedullary junction (Fig. 4*D*). Thus, although intermittent pharmacologic ACTH stimulation partially limits

adrenocortical apoptosis and macrophage accumulation, it fails to sustain steroidogenic capacity and ultimately slows functional recovery.

We then tested whether sustained, endogenous ACTH signaling during the period of glucocorticoid exposure prevents GIAI (Model 3, Fig. S1). We created Sim1^{Cre}:GR$^{fl/fl}$ mice (HGRKO), which have reduced hypothalamic glucocorticoid receptor expression and exhibit constitutively elevated *Crh* mRNA content and plasma ACTH and corticosterone concentrations[27]. Cre-negative littermates (HGRWT) were used as controls. Mice were treated for either 4 days or 8 weeks with DEX. HPA axis activity was assessed pre-treatment and on chronic DEX (8+0) in the unstressed state, following physical restraint, and after cosyntropin stimulation. On long-term DEX treatment (8+0), GR immunoreactivity was present in 94% of PVH neurons of HGRWT mice vs. 23% in HGRKO mice (Fig. S6*A*, *B*). *Crh* expression in the PVH was suppressed in these same DEX-treated HGRWT (49±12 AU) but not HGRKO animals (244±2.2 AU; Fig. S6*C, D*). GR was thus mostly deleted from the PVH, which conferred resistance DEX-induced feedback inhibition of *Crh* mRNA expression.

Apoptosis was uniformly rare in DN (0.63±0.19%) and short-term DEX-treated HGRKO glands (1.7±0.9%, p=0.74), compared to the increase found in DEX-treated WT glands (11±0.8%, p<0.0001 vs. DN and 4D DEX HGRKO; Fig. 5A, *B*). HGRKO mice had higher basal ACTH concentrations than HGRWT controls (470±76 vs. 104±55 pg/mL, $p<0.05$) that were not suppressed on long-term DEX (385±64 vs. 0±0 pg/mL; $p<0.01$; Fig. 5*C*). Pre-treatment basal and stimulated CORT levels were expectedly higher in HGRKO compared to HGRWT mice (Fig. 5*D*). On long-term DEX, basal, restraint- and cosyntropin-stimulated CORT were all markedly suppressed in HGRWT mice, whereas these levels remained high in HGRKO animals (basal: 1.5±0.98 vs. 14±1.6 µg/dL; restraint: 1.9±1.6 vs. 33±4.5 µg/dL; cosyntropin-stimulated: 1.1±0.62 vs. 33±3.9 µg/dL; $p<0.01$–0.001). Adrenal mass and morphology were normal in HGRKO animals, and these glands notably lacked the large clusters of AMs observed in HGRWT controls (Fig. 5E-

I). Sustained, CRH-driven, endogenous ACTH signaling during long-term DEX treatment thus prevents GIAI and cortical atrophy.

Discussion

Using a murine model of GIAI, we found that hypothalamic-pituitary function rapidly recovered after cessation of chronic glucocorticoids, whereas adrenal suppression persisted for up to 8 weeks. DEX-exposed adrenals exhibited marked cortical atrophy and infiltration with large, lipid-laden macrophages. Even after accounting for these macrophages, CORT production was disproportionately low relative to the size of the adrenal cortex, suggesting that post-withdrawal GIAI involves both adrenocortical cell loss and steroidogenic or secretory dysfunction. The provision of continuous, CRH-driven, endogenous ACTH signaling to the adrenal during long-term DEX treatment preserved adrenal size, morphology, and function. These results identify the adrenal as the principal site of prolonged dysfunction after long-term glucocorticoid treatment and point to sustained trophic stimulation of the gland as a promising therapeutic strategy to prevent GIAI.

Consistent with our findings, prior rodent studies have shown that hypothalamic-pituitary function recovers within one week of discontinuing short- to moderate-term glucocorticoid treatment (5-30 days)[23-25]. We extended treatment to a duration known to cause protracted GIAI in humans, making the rapid central recovery observed in our model particularly striking. Notably, the 1965 study that established the paradigm of post-withdrawal central suppression included only six patients with exogenous glucocorticoid exposure. Because ACTH could not be directly measured, circulating levels were inferred from the corticosterone responses of hypophysectomized rats injected with patient plasma, three standard doses of ACTH, or saline[14,15]. Another frequently cited study assessed HPA axis function just 24 hours (1-2 biological half-lives) after the final glucocorticoid dose[16]. ACTH suppression in this context could

therefore reflect direct, glucocorticoid-mediated feedback inhibition on the hypothalamus and pituitary rather than delayed central axis recovery. Interestingly, ACTH levels are elevated at the morning hydrocortisone trough in patients treated for congenital adrenal hyperplasia[21,22]. This suggests that central axis activity recovers rapidly after glucocorticoid withdrawal in at least some patients who require chronic, suppressive therapy. Together, the methodological limitations of earlier clinical studies and our demonstration of rapid hypothalamic–pituitary recovery in mice call into question the long-standing assumption that delayed central recovery is the primary determinant of prolonged HPA axis suppression after chronic glucocorticoid therapy.

The rapid post-withdrawal central recovery found in our study encouraged us to investigate mechanisms of GIAI at the adrenal level. Since ACTH is a well-established trophic factor for the zF[7,8], the time required for cellular regeneration from DEX-induced cortical atrophy is an intuitive explanation for persistently low CORT secretion after glucocorticoid withdrawal despite supraphysiologic ACTH stimulation. The adult zona fasciculata is considered a moderately proliferative tissue with a turnover rate of 120 days in mice[43,44]. While this is longer than the 8 weeks required for functional recovery in our study, more rapid renewal would be expected in states of increased ACTH stimulation, as occurs after DEX withdrawal[45]. Interestingly, we found that adrenal mass recovered more rapidly than steroidogenic function. This is consistent with prior studies that demonstrated that CORT levels and steroidogenic pathway gene expression were low one week after discontinuing short- to moderate-term glucocorticoids despite normalization of adrenal weights[23-25]. Using quantitative morphometry, we further demonstrated that this dissociation between adrenal size and function persisted even after accounting for the DEX-induced expansion of large, lipid-laden adrenal macrophages. Together, these findings suggest that post-withdrawal GIAI reflects not only adrenocortical cell loss but also a persistent defect in CORT biosynthesis or secretion, the mechanisms of which will be a focus of future studies.

While Wylie et al. noted accumulation of apoptotic bodies “within phagosomes of ‘histiocytes’” after short-term glucocorticoid treatment[7], adrenal macrophage accumulation has not been reported after long-term glucocorticoid therapy. Large AMs in our model share multiple features with adrenal macrophages described in acute and chronic stress states. They express classical macrophage markers, such as CD68, F4/80 and Cd11c, and are intensely autofluorescent due to lipid accumulation[40,46-48]. Male murine adrenal macrophages are also long-lived[48], consistent with our continued detection of AMs at least 8 weeks after DEX withdrawal. The AMs in the present study most strikingly differ from typical adrenal macrophages in both their large size and apparent multinucleation. Morphologically similar adrenal macrophages have been described in aged, male *Znrf3* knockout mice, which undergo early adrenocortical hyperplasia followed by senescence[49]. It is therefore plausible that adrenal macrophages undergo expansion, fusion, and multinucleation when the demand for phagocytic clearance is high, as has been reported in adipose, ovary and bone tissues[50-52]. Interestingly, Xu et al. reported that adrenal macrophages in atherogenic conditions restrict glucocorticoid production via Trem2-dependent paracrine suppression of steroidogenic acute regulatory protein (StAR), the rate limiting enzyme in CORT biosynthesis, in neighboring zona fasciculata cells[40]. Since AMs in our model strongly express *Trem2,* further work is needed to determine if they contribute to GIAI via a similar paracrine signaling mechanism.

Most importantly, our finding that central HPA axis signaling recovers rapidly after cessation of chronic glucocorticoid therapy has enabled us to begin development of new, adrenally targeted strategies to prevent GIAI. Presently, no therapies exist that prevent or accelerate recovery from GIAI, in part because of the prevailing assumption that prolonged hypothalamic-pituitary suppression after steroid withdrawal will inevitably lead to adrenal dysfunction, even if glandular integrity could be preserved during treatment. By demonstrating that hypothalamic pituitary signaling is rapidly restored following glucocorticoid withdrawal, our data challenge this

longstanding dogma and reorient translational efforts toward the adrenal, which is a far more accessible therapeutic target than the hypothalamus or pituitary.

Consistent with this framework, we have shown that sustained, CRH-driven ACTH signaling preserves adrenal function and architecture during chronic glucocorticoid treatment. The endocrine phenotype in this HGRKO model arises from hypothalamic GR deletion, which disrupts the principal mechanism by which glucocorticoids exert negative feedback on the HPA axis. Accordingly, the HGRKO model is not itself directly translatable but instead serves as an important proof of principle that maintenance of physiologic trophic support to the adrenal during long-term glucocorticoid therapy prevents GIAI. The constitutive nature of this model precluded assessment of whether full HPA axis function is restored following both glucocorticoid withdrawal and reversal of the genetic manipulation. Although this will be an important consideration for future attempts to replicate this model pharmacologically, we do not anticipate it to represent a major limitation given our finding that hypothalamic-pituitary suppression reverses within one week of DEX withdrawal even in wild-type mice.

The resistance of HGRKO mice to GIAI further suggests that CRH stimulation can overcome glucocorticoid mediated feedback inhibition at the level of the pituitary. This effect cannot be attributed to unintended GR deletion or “leaky” Cre recombinase activity in corticotropes, as intact GR expression in ACTH-positive anterior pituitary cells of HGRKO mice has been previously demonstrated[27]. The ability of CRH signaling to dominate over glucocorticoid feedback at the corticotrope has substantial translational relevance for the development of CRH-based strategies to prevent GIAI, which may be superior to approaches relying solely on ACTH. In contrast to the robust rescue observed in HGRO mice, we found that adrenal function recovered more slowly in wild-type mice treated with dexamethasone and cosyntropin vs. with dexamethasone alone. Similarly, combination therapy with intramuscular ACTH and glucocorticoids produced more severe HPA axis suppression in patients with rheumatologic

disease compared to those treated with glucocorticoids alone[53]. These failures may reflect, in part, the short half-lives of ACTH and cosyntropin, both of which are estimated at 10-30 minutes[54,55]. However, even in patients with Cushing syndrome, in whom autonomous CRH or ACTH secretion is sustained, adrenal function recovers more rapidly after resection of an ectopic, CRH-producing tumor than an ACTH-secreting adenoma[56] . In glucocorticoid treated rats, pulsatile but not continuous ACTH infusion restored CORT secretion and expression of key steroidogenic genes[57,58]. While we were unable to assess ultradian ACTH dynamics in HGRKO mice due to blood volume constraints and the stress associated with serial sampling, CORT secretion in these mice follows a normal circadian pattern[27]. We have also previously shown that continuous infusion of CRH restores circadian ACTH and CORT rhythms in CRH knockout mice[29]. Since the pituitary resides outside the blood brain barrier, systemic administration of long-acting CRH or a CRH-receptor agonist concurrent with chronic glucocorticoid therapy may thus maintain physiologic ACTH stimulation of the adrenal and prevent GIAI.

As a potential limitation, this study only included male mice to minimize biological variability across a broad, exploratory survey of HPA axis recovery. While there are no reported sex differences in the risk, severity, or duration of GIAI in humans[10,59-61], HPA axis responsiveness, rates of adrenocortical turnover, and adrenal macrophage populations are all sexually dimorphic in rodents[49,62-68]. Future studies will specifically investigate sex differences in the mechanisms of post-withdrawal GIAI and time to HPA axis recovery in this preclinical model. Additionally, sample sizes were relatively modest to permit interrogation of HPA axis function at multiple timepoints after chronic glucocorticoid treatment. Since we examined HPA axis function in the stimulated state, as is done to clinically diagnose adrenal insufficiency, key analyses were all still adequately powered. Nonetheless, subsequent mechanistic studies will include larger cohorts of animals now that biologically relevant timepoints have been identified.

In conclusion, our findings demonstrate that post-withdrawal GIAI arises primarily from adrenal dysfunction rather than delayed hypothalamic-pituitary recovery. This prolonged adrenal suppression, driven by both adrenocortical cell loss and impaired steroid synthesis or secretion, is prevented by maintaining sustained trophic stimulation of the adrenal during glucocorticoid exposure. These results establish the adrenal as the principal locus of post-withdrawal GIAI and an accessible target for therapeutic intervention. Pharmacologic strategies that maintain physiologic adrenal stimulation could prevent GIAI, thereby reducing the morbidity associated with one of the most widely prescribed drug classes while preserving their therapeutic efficacy.

Acknowledgments

We thank Drs. David Breault, Kleiton Borges, and Mesut Berber for their input on this project and assistance processing adrenal tissue, identifying zonal markers, and performing thick, floating section immunofluorescence. We also thank Suzanne White from the BIDMC Histology core for preparing and sectioning all FFPE specimens, including working closely with the author (LG) to isolate the PVH in mouse brains.

Data availability

Original data generated and analyzed during this study are included in this published article or in the data repositories listed in References.

References

1. Fardet L, Petersen I, Nazareth I. Prevalence of long-term oral glucocorticoid prescriptions in the UK over the past 20 years. *Rheumatology (Oxford).* 2011;50(11):1982-1990.

2. Overman RA, Yeh JY, Deal CL. Prevalence of oral glucocorticoid usage in the United States: a general population perspective. *Arthritis Care Res (Hoboken).* 2013;65(2):294-298.
3. Daley-Yates P, Brealey N, Thomas S, et al. Therapeutic index of inhaled corticosteroids in asthma: A dose-response comparison on airway hyperresponsiveness and adrenal axis suppression. *Br J Clin Pharmacol.* 2021;87(2):483-493.
4. Woods CP, Argese N, Chapman M, et al. Adrenal suppression in patients taking inhaled glucocorticoids is highly prevalent and management can be guided by morning cortisol. *European journal of endocrinology.* 2015;173(5):633-642.
5. Lam LH, Sugarman JL. Adrenal Suppression With Chronic Topical Corticosteroid Use in Psoriasis Patients. *J Drugs Dermatol.* 2016;15(8):945-948.
6. Keller-Wood ME, Dallman MF. Corticosteroid inhibition of ACTH secretion. *Endocrine reviews.* 1984;5(1):1-24.
7. Wyllie AH, Kerr JF, Currie AR. Cellular events in the adrenal cortex following ACTH deprivation. *The Journal of pathology.* 1972;106(1):Pix.
8. Wyllie AH, Kerr JF, Macaskill IA, Currie AR. Adrenocortical cell deletion: the role of ACTH. *The Journal of pathology.* 1973;111(2):85-94.
9. Younes AK, Younes NK. Recovery of steroid induced adrenal insufficiency. *Translational pediatrics.* 2017;6(4):269-273.
10. Livanou T, Ferriman D, James VH. Recovery of hypothalamo-pituitary-adrenal function after corticosteroid therapy. *Lancet (London, England).* 1967;2(7521):856-859.
11. Beuschlein F, Else T, Bancos I, et al. European Society of Endocrinology and Endocrine Society Joint Clinical Guideline: Diagnosis and therapy of glucocorticoid-induced adrenal insufficiency. *European journal of endocrinology.* 2024;190(5):G25-g51.
12. Ebrahimi F, Widmer A, Wagner U, et al. Association of adrenal insufficiency with patient-oriented health-care outcomes in adult medical inpatients. *European journal of endocrinology.* 2019;181(6):701-709.
13. Mebrahtu TF, Morgan AW, Keeley A, Baxter PD, Stewart PM, Pujades-Rodriguez M. Dose dependency of iatrogenic glucocorticoid excess and adrenal insufficiency and mortality: a cohort study in England. *The Journal of clinical endocrinology and metabolism.* 2019;104(9):3757-3767.
14. Graber AL, Ney RL, Nicholson WE, Island DP, Liddle GW. NATURAL HISTORY OF PITUITARY-ADRENAL RECOVERY FOLLOWING LONG-TERM SUPPRESSION WITH CORTICOSTEROIDS. *The Journal of clinical endocrinology and metabolism.* 1965;25:11-16.
15. Ney RL, Shimizu N, Nicholson WE, Island DP, Liddle GW. CORRELATION OF PLASMA ACTH CONCENTRATION WITH ADRENOCORTICAL RESPONSE IN NORMAL HUMAN SUBJECTS, SURGICAL PATIENTS, AND PATIENTS WITH CUSHING'S DISEASE. *The Journal of clinical investigation.* 1963;42(11):1669-1677.
16. Schlaghecke R, Kornely E, Santen RT, Ridderskamp P. The effect of long-term glucocorticoid therapy on pituitary-adrenal responses to exogenous corticotropin-releasing hormone. *The New England journal of medicine.* 1992;326(4):226-230.
17. Rao PS. Corticosteroids. In: Wexler P, ed. *Encyclopedia of Toxicology (Second Edition).* New York: Elsevier; 2005:669-670.
18. Avgerinos PC, Chrousos GP, Nieman LK, Oldfield EH, Loriaux DL, Cutler GB, Jr. The corticotropin-releasing hormone test in the postoperative evaluation of patients with cushing's syndrome. *The Journal of clinical endocrinology and metabolism.* 1987;65(5):906-913.
19. Avgerinos PC, Nieman LK, Oldfield EH, et al. The effect of pulsatile human corticotropin-releasing hormone administration on the adrenal insufficiency that follows cure of

Cushing's disease. *The Journal of clinical endocrinology and metabolism.* 1989;68(5):912-916.

20. Gomez MT, Magiakou MA, Mastorakos G, Chrousos GP. The pituitary corticotroph is not the rate limiting step in the postoperative recovery of the hypothalamic-pituitary-adrenal axis in patients with Cushing syndrome. *The Journal of clinical endocrinology and metabolism.* 1993;77(1):173-177.
21. Dauber A, Feldman HA, Majzoub JA. Nocturnal Dexamethasone versus Hydrocortisone for the Treatment of Children with Congenital Adrenal Hyperplasia. *Int J Pediatr Endocrinol.* 2010;2010.
22. Mallappa A, Sinaii N, Kumar P, et al. A phase 2 study of Chronocort, a modified-release formulation of hydrocortisone, in the treatment of adults with classic congenital adrenal hyperplasia. *The Journal of clinical endocrinology and metabolism.* 2015;100(3):1137-1145.
23. Spiga F, Zhao Z, Lightman SL. Prolonged treatment with the synthetic glucocorticoid methylprednisolone affects adrenal steroidogenic function and response to inflammatory stress in the rat. *Brain Behav Immun.* 2020;87:703-714.
24. Calogero AE, Kamilaris TC, Johnson EO, Tartaglia ME, Chrousos G. Recovery of the rat hypothalamic-pituitary-adrenal axis after discontinuation of prolonged treatment with the synthetic glucocorticoid agonist dexamethasone. *Endocrinology.* 1990;127(4):1574-1579.
25. Duncan PJ, McClafferty H, Nolan O, et al. Corticotroph isolation from Pomc-eGFP mice reveals sustained transcriptional dysregulation characterising a mouse model of glucocorticoid-induced suppression of the hypothalamus-pituitary-adrenal axis. *J Neuroendocrinol.* 2022;34(7):e13165.
26. Tronche F, Kellendonk C, Kretz O, et al. Disruption of the glucocorticoid receptor gene in the nervous system results in reduced anxiety. *Nature genetics.* 1999;23(1):99-103.
27. Laryea G, Schütz G, Muglia LJ. Disrupting hypothalamic glucocorticoid receptors causes HPA axis hyperactivity and excess adiposity. *Molecular endocrinology (Baltimore, Md).* 2013;27(10):1655-1665.
28. Bachmanov AA, Reed DR, Beauchamp GK, Tordoff MG. Food intake, water intake, and drinking spout side preference of 28 mouse strains. *Behav Genet.* 2002;32(6):435-443.
29. Muglia LJ, Jacobson L, Weninger SC, et al. Impaired diurnal adrenal rhythmicity restored by constant infusion of corticotropin-releasing hormone in corticotropin-releasing hormone-deficient mice. *The Journal of clinical investigation.* 1997;99(12):2923-2929.
30. Jacobson L, Muglia LJ, Weninger SC, Pacák K, Majzoub JA. CRH deficiency impairs but does not block pituitary-adrenal responses to diverse stressors. *Neuroendocrinology.* 2000;71(2):79-87.
31. Farny NG, Hurt JA, Silver PA. Definition of global and transcript-specific mRNA export pathways in metazoans. *Genes Dev.* 2008;22(1):66-78.
32. Hurt JA, Obar RA, Zhai B, Farny NG, Gygi SP, Silver PA. A conserved CCCH-type zinc finger protein regulates mRNA nuclear adenylation and export. *J Cell Biol.* 2009;185(2):265-277.
33. Liu X, Oh S, Kirschner MW. The uniformity and stability of cellular mass density in mammalian cell culture. *Front Cell Dev Biol.* 2022;10:1017499.
34. Kafri R, Levy J, Ginzberg MB, Oh S, Lahav G, Kirschner MW. Dynamics extracted from fixed cells reveal feedback linking cell growth to cell cycle. *Nature.* 2013;494(7438):480-483.
35. Leng S, Pignatti E, Khetani RS, et al. β-Catenin and FGFR2 regulate postnatal rosette-based adrenocortical morphogenesis. *Nat Commun.* 2020;11(1):1680.
36. Paul A, Laufer E. Endogenous biotin as a marker of adrenocortical cells with steroidogenic potential. *Molecular and cellular endocrinology.* 2011;336(1-2):133-140.

37. Sakr N, Glazova O, Shevkova L, et al. Characterizing and Quenching Autofluorescence in Fixed Mouse Adrenal Cortex Tissue. *Int J Mol Sci.* 2023;24(4).
38. Wentworth JM, Naselli G, Brown WA, et al. Pro-inflammatory CD11c+CD206+ adipose tissue macrophages are associated with insulin resistance in human obesity. *Diabetes.* 2010;59(7):1648-1656.
39. Wu H, Gower RM, Wang H, et al. Functional role of CD11c+ monocytes in atherogenesis associated with hypercholesterolemia. *Circulation.* 2009;119(20):2708-2717.
40. Xu Y, Patterson MT, Dolfi B, et al. Adrenal gland macrophages regulate glucocorticoid production through Trem2 and TGF-β. *JCI Insight.* 2024;9(14).
41. Ganguly S, Rosenthal SB, Ishizuka K, et al. Lipid-associated macrophages' promotion of fibrosis resolution during MASH regression requires TREM2. *Proceedings of the National Academy of Sciences of the United States of America.* 2024;121(35):e2405746121.
42. Dallman MF. Control of adrenocortical growth in vivo. *Endocrine research.* 1984;10(3-4):213-242.
43. Freedman BD, Kempna PB, Carlone DL, et al. Adrenocortical zonation results from lineage conversion of differentiated zona glomerulosa cells. *Developmental cell.* 2013;26(6):666-673.
44. Kataoka Y, Ikehara Y, Hattori T. Cell proliferation and renewal of mouse adrenal cortex. *J Anat.* 1996;188 (Pt 2)(Pt 2):375-381.
45. Yates R, Katugampola H, Cavlan D, et al. Adrenocortical development, maintenance, and disease. *Curr Top Dev Biol.* 2013;106:239-312.
46. Hume DA, Halpin D, Charlton H, Gordon S. The mononuclear phagocyte system of the mouse defined by immunohistochemical localization of antigen F4/80: macrophages of endocrine organs. *Proc Natl Acad Sci U S A.* 1984;81(13):4174-4177.
47. González-Hernández JA, Bornstein SR, Ehrhart-Bornstein M, Geschwend JE, Adler G, Scherbaum WA. Macrophages within the human adrenal gland. *Cell and Tissue Research.* 1994;278(2):201-205.
48. O'Brien CJO. Macrophage Regulation of Hypothalamic-Pituitary-Adrenal and Gonadal Axis Homeostasis and Hormonal Output. *Biomed J.* 2025:100866.
49. Warde KM, Smith LJ, Liu L, et al. Senescence-induced immune remodeling facilitates metastatic adrenal cancer in a sex-dimorphic manner. *Nat Aging.* 2023;3(7):846-865.
50. Lazarov T, Juarez-Carreño S, Cox N, Geissmann F. Physiology and diseases of tissue-resident macrophages. *Nature.* 2023;618(7966):698-707.
51. Foley KG, Pritchard MT, Duncan FE. Macrophage-derived multinucleated giant cells: hallmarks of the aging ovary. *Reproduction.* 2021;161(2):V5-v9.
52. Braune J, Lindhorst A, Fröba J, et al. Multinucleated Giant Cells in Adipose Tissue Are Specialized in Adipocyte Degradation. *Diabetes.* 2021;70(2):538-548.
53. Carter ME, James VH. An attempt at combining corticotrophin with long-term corticosteroid therapy. With a view to preserving hypothalmic-pituitary-adrenal function. *Ann Rheum Dis.* 1970;29(4):409-414.
54. Hamilton DD, Cotton BA. Cosyntropin as a diagnostic agent in the screening of patients for adrenocortical insufficiency. *Clin Pharmacol.* 2010;2:77-82.
55. Furman BL. Cosyntropin. In: Enna SJ, Bylund DB, eds. *xPharm: The Comprehensive Pharmacology Reference.* New York: Elsevier; 2007:1-3.
56. Lois KB, Santhakumar A, Vaikkakara S, et al. Phaeochromocytoma and ACTH-dependent cushing's syndrome: tumour crf secretion can mimic pituitary cushing's disease. *Clin Endocrinol (Oxf).* 2016;84(2):177-184.
57. Spiga F, Waite EJ, Liu Y, Kershaw YM, Aguilera G, Lightman SL. ACTH-dependent ultradian rhythm of corticosterone secretion. *Endocrinology.* 2011;152(4):1448-1457.
58. Liu Y, Smith LI, Huang V, et al. Transcriptional regulation of episodic glucocorticoid secretion. *Molecular and cellular endocrinology.* 2013;371(1-2):62-70.

59. Broersen LH, Pereira AM, Jørgensen JO, Dekkers OM. Adrenal Insufficiency in Corticosteroids Use: Systematic Review and Meta-Analysis. *The Journal of clinical endocrinology and metabolism.* 2015;100(6):2171-2180.
60. Prete A, Bancos I. Glucocorticoid induced adrenal insufficiency. *BMJ.* 2021;374:n1380.
61. Prete A, Paragliola RM, Bottiglieri F, et al. Factors predicting the duration of adrenal insufficiency in patients successfully treated for Cushing disease and nonmalignant primary adrenal Cushing syndrome. *Endocrine.* 2017;55(3):969-980.
62. Gao X, Yamazaki Y, Tezuka Y, et al. Gender differences in human adrenal cortex and its disorders. *Molecular and cellular endocrinology.* 2021;526:111177.
63. Duncko R, Kiss A, Skultétyová I, Rusnák M, Jezová D. Corticotropin-releasing hormone mRNA levels in response to chronic mild stress rise in male but not in female rats while tyrosine hydroxylase mRNA levels decrease in both sexes. *Psychoneuroendocrinology.* 2001;26(1):77-89.
64. Viau V, Bingham B, Davis J, Lee P, Wong M. Gender and puberty interact on the stress-induced activation of parvocellular neurosecretory neurons and corticotropin-releasing hormone messenger ribonucleic acid expression in the rat. *Endocrinology.* 2005;146(1):137-146.
65. Goel N, Bale TL. Sex differences in the serotonergic influence on the hypothalamic-pituitary-adrenal stress axis. *Endocrinology.* 2010;151(4):1784-1794.
66. Grabek A, Dolfi B, Klein B, Jian-Motamedi F, Chaboissier MC, Schedl A. The Adult Adrenal Cortex Undergoes Rapid Tissue Renewal in a Sex-Specific Manner. *Cell Stem Cell.* 2019;25(2):290-296.e292.
67. Hammer GD, Basham KJ. Stem cell function and plasticity in the normal physiology of the adrenal cortex. *Molecular and cellular endocrinology.* 2021;519:111043.
68. Dolfi B, Gallerand A, Firulyova MM, et al. Unravelling the sex-specific diversity and functions of adrenal gland macrophages. *Cell reports.* 2022;39(11):110949.

Figures and Tables

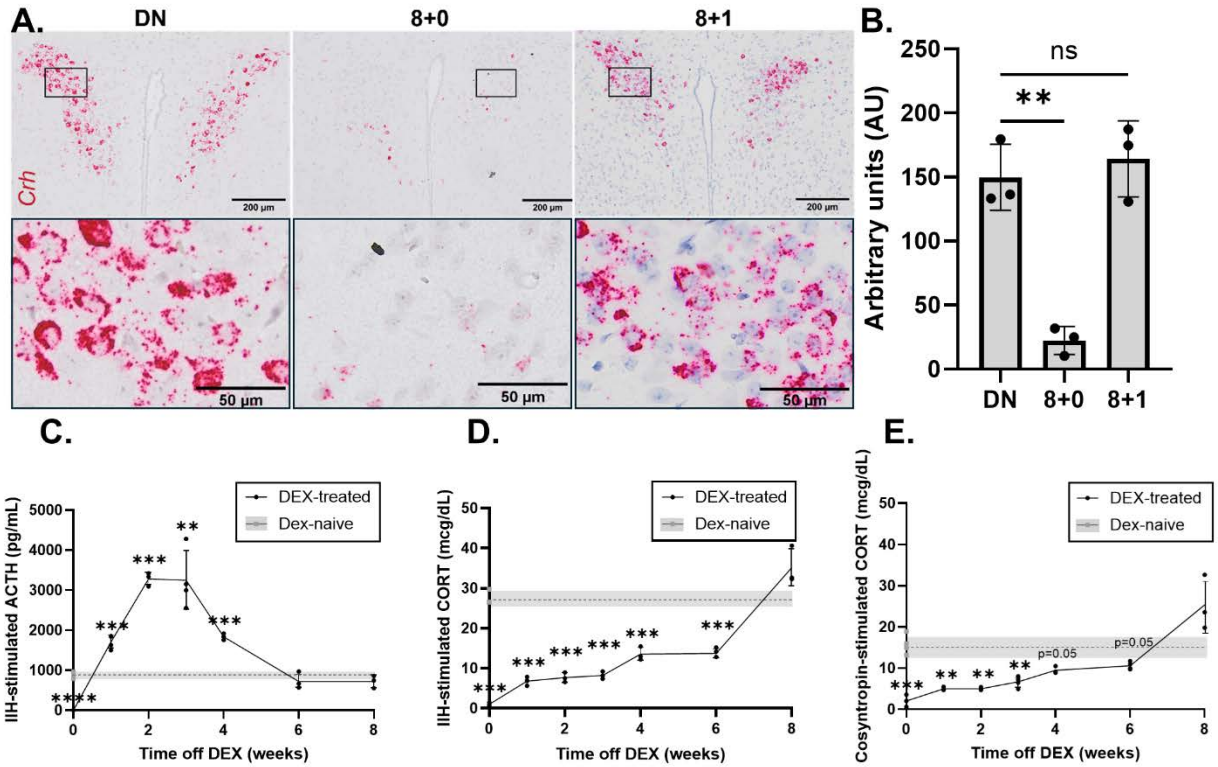

Figure 1. **Corticosterone (CORT) secretion is suppressed for up to 8 weeks after discontinuing long-term DEX despite rapid hypothalamic-pituitary recovery.** A) *In situ* hybridization (RNAScope) for basal *Crh* (red) in the paraventricular nucleus (PVH) of the hypothalamus in DEX-naïve (DN) animals and those treated with 8 weeks DEX both immediately prior to (8+0) and 1-week post-withdrawal (8+1; top row, scale bar=200 microns). Nuclei are labeled by hematoxylin (purple). Magnification of region within the black box is shown directly below (bottom row, scale bar=50 microns). B) Quantification of *Crh* mRNA expression from RNAScope images of the PVH from DN, 8+0, and 8+1 animals (n=3). $p<0.001$ by 1-way ANOVA. Recovery of insulin-stimulated plasma C) ACTH and D) CORT and E) cosyntropin-stimulated CORT levels 0-8 weeks after withdrawal of an 8-week DEX course. Data shown as individual mice with mean (connecting line) ± SEM (error bars). Gray bar (mean± SEM)

indicates the reference range for adult, male, wildtype, untreated (DEX-naïve or DN) controls (n=4-8). * denotes p<0.05, ** p<0.01, *** p<0.001, and ****p<0.0001 vs. DN.

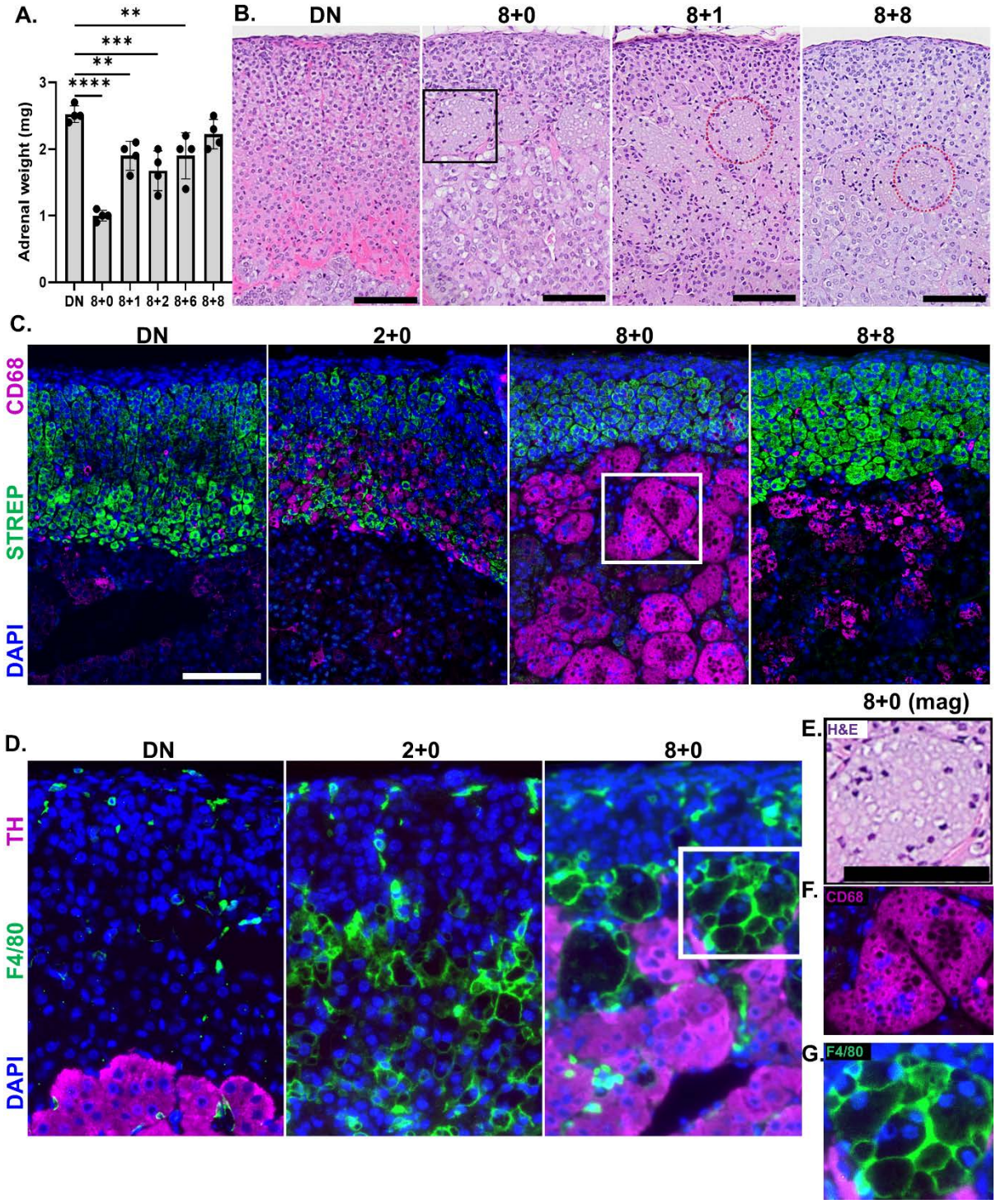

Figure 2. Long-term DEX induces adrenocortical atrophy with accumulation of large macrophage clusters that persist for at least 8 weeks post-withdrawal. A) DEX-treated

adrenals weigh significantly less than DN controls through 6 weeks post-withdrawal. $P<0.0001$ by one-way ANOVA; * indicates $p<0.05$, ** $p<0.01$, *** $p<0.001$, and ****$p<0.0001$ vs. DN. B) Hematoxylin and eosin staining reveals large, poorly defined, vacuolated structures with decreased nuclear density at the corticomedullary junction in DEX-exposed adrenals that persist through 8-weeks post-withdrawal. Representative structures (outlined with red, dashed circles) correspond with clusters of cells that are positive for the classical macrophage markers C) CD68 and D) F4/80. C) Immunofluorescence for CD68 (magenta) with DAPI (blue) and 488-streptavidin (green) counterstains, the latter of which labels all biotin-rich cells of the adrenal cortex. Representative images shown for DN adrenals, those on DEX for 2-8 weeks (e.g. 2+0 to 8+0), as well as one (8+1) and eight (8+8) weeks after an 8-week DEX course. D) Immunofluorescence for the mouse macrophage marker F4/80 (green) and medullary marker tyrosine hydroxylase (TH; magenta) in DN and DEX-exposed adrenals (2+0 and 8+0). Magnification of representative macrophages in 8+0 glands from E) H&E and immunostaining for F) CD68 and G) F4/80. All staining performed with TrueBlack lipofuscin autofluorescence quencher (C, D, F, and G).

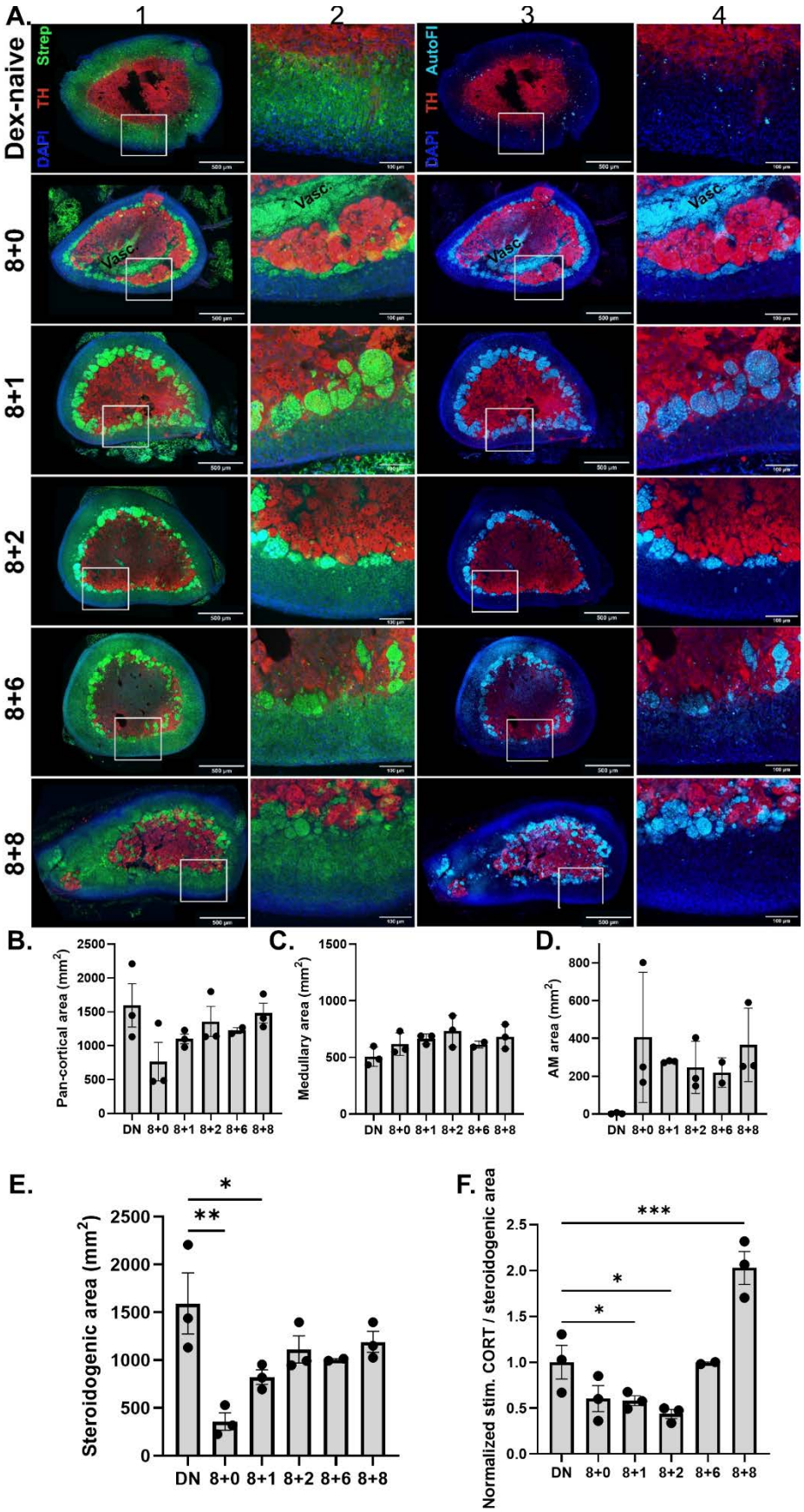
A.
1
2
3
4
Dex-naive
8+0
8+1
8+2
8+6
8+8
DAPI
TH
Strep
AutoFl
Vasc.
B.
Pan-cortical area (mm²)
C.
Medullary area (mm²)
D.
AM area (mm²)
DN
8+0
8+1
8+2
8+6
8+8
E.
Steroidogenic area (mm²)
F.
Normalized stim. CORT / steroidogenic area

Figure 3. Stimulated CORT secretion is disproportionately low relative to adrenocortical cell mass for at least 2 weeks after withdrawal of long-term DEX. A) IF without TrueBlack for tyrosine hydroxylase (TH, red) DAPI (blue) and 488-streptavidin (green; columns 1 and 2) counterstains. Adrenal macrophages (AMs) were detected by autofluorescence (cyan; columns 3 and 4). Mice were either untreated (DN) or treated for 8 weeks DEX followed by withdrawal for 0-8 weeks (8+0, 8+1, 8+2, 8+6, and 8+8). Shown as 100 µM-thick, whole adrenal slices (columns 1 and 3, scale bar=500 microns) with magnification of the region in the white box (columns 2 and 4, scale bar=100 microns). Columns 1 and 2 imaged at wavelengths 405 nm, 488 nm, and 647 nm; columns 3 and 4 imaged at wavelengths 405 nm, 440 nm, and 647 nm. Morphometric analysis of B) pan-cortical area, which includes both streptavidin-positive and autofluorescent regions ($p=0.18$ by one-way ANOVA), C) Autofluorescent AM area ($p=0.18$), D) steroidogenic cell type area, calculated as pan-cortical area minus AMs ($p<0.01$), and E) medullary (TH- positive) area ($p=0.17$ by one-way ANOVA). F) Ratio of steroidogenic cell type area to cosyntropin-stimulated CORT secretion, normalized to DN controls. * $p<0.05$, ** $p<0.01$, *** $p<0.001$ vs. DN (B-F)

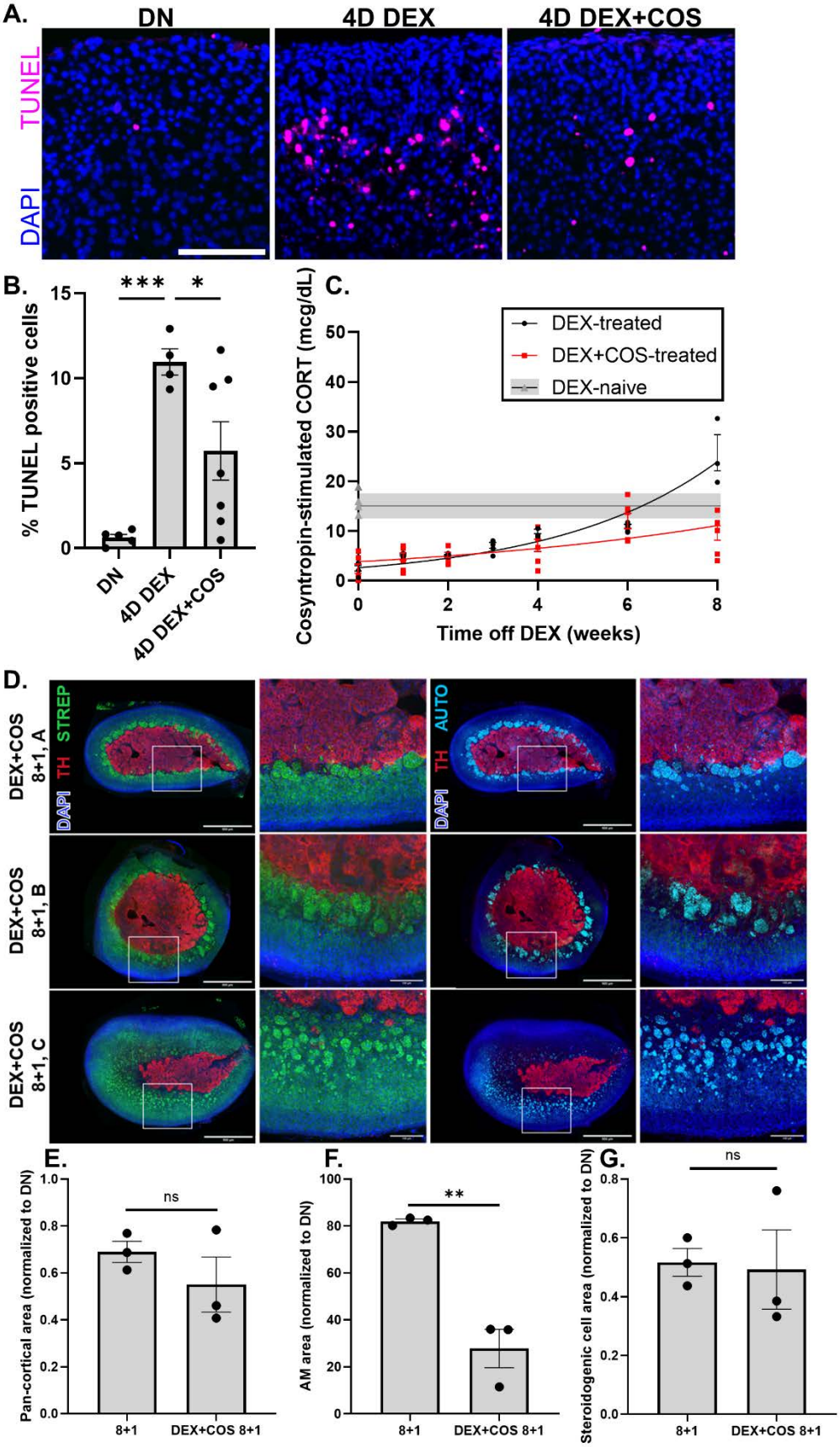
A.
DN
4D DEX
4D DEX+COS
TUNEL
DAPI
B.
% TUNEL positive cells
***
*
DN
4D DEX
4D DEX+COS
C.
Cosyntropin-stimulated CORT (mcg/dL)
DEX-treated
DEX+COS-treated
DEX-naive
Time off DEX (weeks)
D.
DEX+COS 8+1, A
DEX+COS 8+1, B
DEX+COS 8+1, C
DAPI TH STREP
DAPI TH AUTO
E.
Pan-cortical area (normalized to DN)
ns
8+1
DEX+COS 8+1
F.
AM area (normalized to DN)
**
8+1
DEX+COS 8+1
G.
Steroidogenic cell area (normalized to DN)
ns
8+1
DEX+COS 8+1

777

Fig. 4. Combined dexamethasone and daily, intraperitoneal cosyntropin (DEX+COS) treatment partially attenuates cortical apoptosis and macrophage accumulation but fails to preserve adrenal function. A) Terminal deoxynucleotidyl transferase dUTP nick end labeling (TUNEL) in adrenals from WT mice treated for 4 days with vehicle (DN), DEX alone (4D DEX), or DEX with daily, intraperitoneal cosyntropin (4D DEX+COS) with B) quantitation. p=-.0012 by one-way ANOVA; p=0.0006 for 4D DEX vs. DN and p=0.04 for DEX+COS vs. 4D DEX. DN and 4D DEX data also shown in Fig. 4*A.* C) After withdrawal, cosyntropin-stimulated CORT secretion recovers more slowly in mice treated for 8 weeks with DEX+COS (red) vs. DEX alone (black). Data shown as individual mice with error bars centered on mean value ± SEM. Gray bar (mean ± SEM) indicates the reference range for adult, male, wildtype, DEX-naïve controls. Stimulated CORT recovery was modeled with exponential functions yielding doubling times of 5.2 weeks after DEX+COS ($Y = 3.8 * e^{0.13X}$ R^2=0.4, red curve) vs. 2.5 weeks after DEX ($Y = 2.6 * e^{0.28X}$; R^2=0.9, black curve). p= 0.0009 by extra sum-of-squares F test. D)Thick, floating section IF without TrueBlack for tyrosine hydroxylase (TH, red), with DAPI (blue), and 488-streptavidin (green) in adrenals withdrawn from long-term DEX+COS (8+1); methods and visualization as per Figs. 3 and 4. All biological replicates are shown given significant morphologic heterogeneity among animals. Morphometric analyses of E) pan-cortical, F) AM, and G) steroidogenic cell type area (all computed as per Figs. 3 and 4) in 8+1 DEX-monotherapy and DEX+COS glands, all normalized to DN controls. Measurements from DN and 8+1 DEX-only adrenals previously shown in Fig. 3. ** p<0.01; ns=not significant.

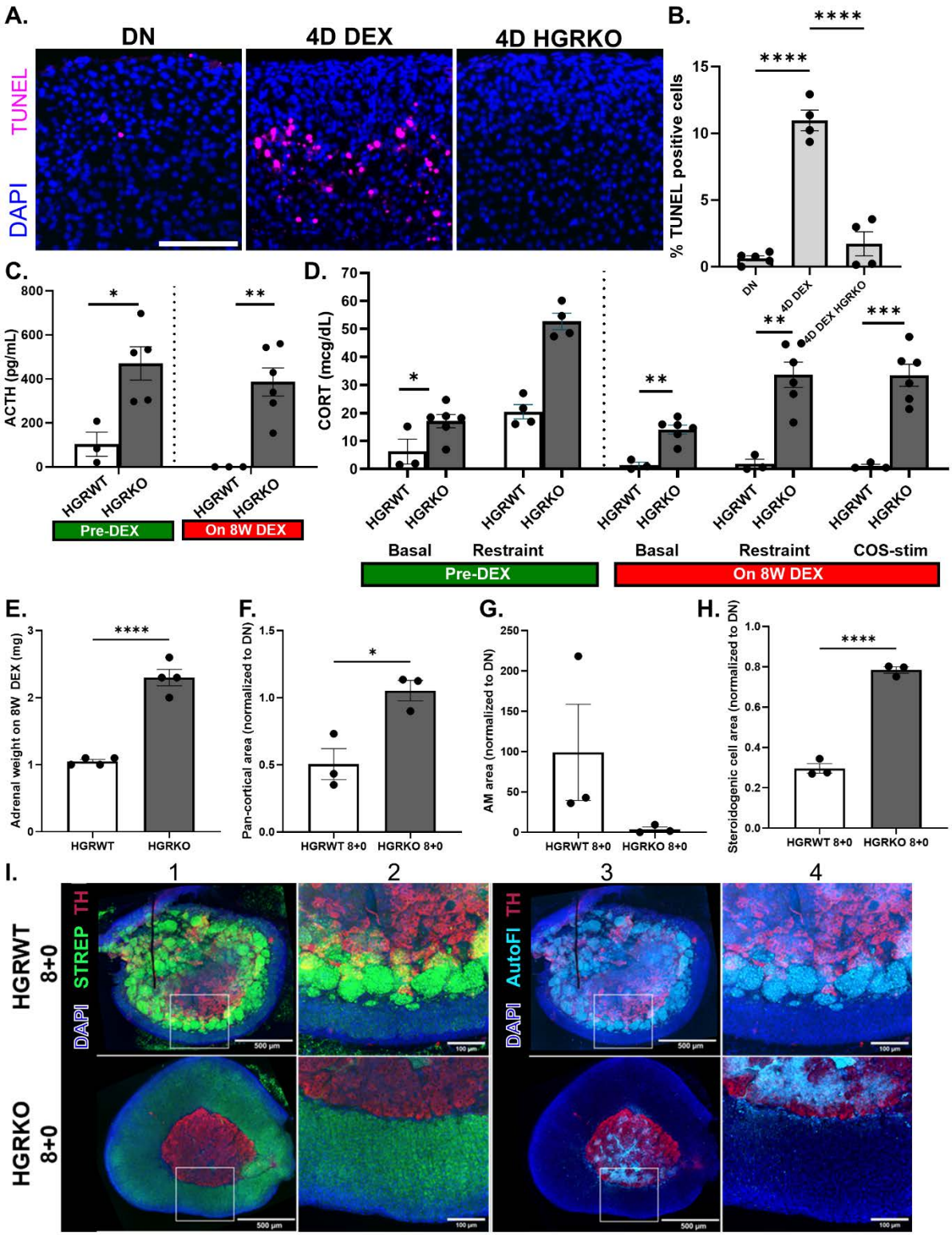

818 **Figure 5. Selective deletion of the hypothalamic glucocorticoid receptor (GR) confers**

819 **protection against DEX-induced adrenal suppression.** A) Short-term (4 days DEX) induces

apoptosis in DEX-treated wild-type (4D DEX) but not Sim1^{Cre}:GR$^{fl/fl}$ (HGRKO) mice, as shown by TUNEL staining (magenta) with B) quantification. $p<0.0001$ by one-way ANOVA, **** denotes $p<0.0001$ for select pairwise comparisons. HGRKO mice and Cre-negative, functionally wild-type littermate controls (HGRWT) mice were then treated with DEX for 8 weeks. Hormonal function was assessed pre-treatment on long-term DEX. C) Basal (unstressed circadian peak) ACTH levels in HGRWT vs. HGRKO animals prior to DEX (left of dashed line) and on 8 weeks of DEX (right of dashed line). $p=0.19$ for DEX status and $p<0.0001$ for genotype by two-way ANOVA. H) CORT secretion in the basal state, following 20 minutes of physical restraint (Restraint), and following cosyntropin stimulation (COS-stim.) in HGRWT vs HGRKO animals, either prior to DEX treatment (left of dashed line) vs. on 8 weeks of DEX (right of dashed line). E) Adrenal weights and morphometric analyses for F) pan-cortical area, G) AM area, and H) steroidogenic cell type area in HGRWT and HGRKO adrenals on long-term DEX (8+0), all computed as per Fig. 3 and normalized to DN adrenals from Fig. 3. I) Representative thick, floating section IF without TrueBlack for tyrosine hydroxylase (TH, red), with DAPI (blue), and 488-streptavidin (green); methods and visualization as per Fig. 3. * $p<0.05$, ** $p<0.01$, *** $p<0.001$, **** $p<0.0001$ by t-test (HGRWT vs. HGRKO (C-H).

Supplemental Figures and Tables

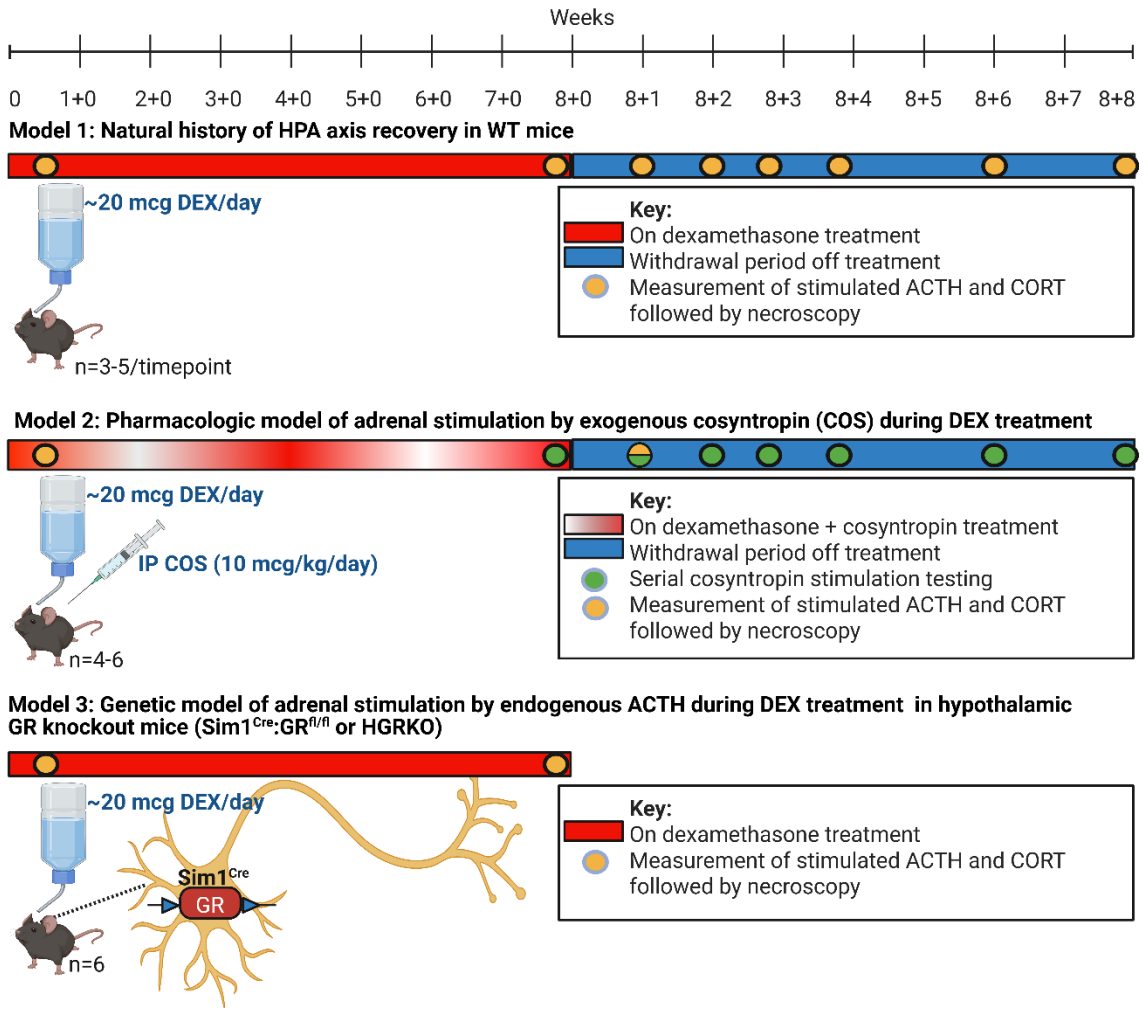

Fig. S1. Experimental design for dexamethasone (DEX) ± cosyntropin (COS) treatment and withdrawal in wild-type (WT; Models 1 and 2) and *Sim1*^{Cre}:*GR*$^{fl/fl}$ (HGRKO; Model 3) mice. In model 1, the natural history of HPA axis recovery after long-term DEX was studied by treating WT mice with 8 weeks of DEX (red bar) followed by serial assessments of axis function and histology at 1-2 week intervals (yellow dots) after DEX was withdrawn (blue bar). Insulin-induced hypoglycemia and cosyntropin stimulation testing were performed on successive days followed by necroscopy. Pharmacologic (model 2) and genetic strategies (model 3) were then studied for their ability to prevent GIAI. In model 2, mice were co-treated for 8 weeks with DEX and cosyntropin, an ACTH analog, followed by cosyntropin-stimulation testing to assess adrenal

function after both agents were withdrawn (green dots). Necroscopy for histologic studies was performed in a separate cohort of mice 1-week post-DEX+COS (8+1; split yellow and green dot). In model 3, HPA axis activity was assessed upon completion of an 8-week DEX course (8+0) in mice with selective hypothalamic deletion of the glucocorticoid receptor (HGRKO), which allows for ongoing, endogenous ACTH secretion on GC therapy. ACTH and CORT were measured in the basal, unstimulated state followed by provocative assessments (restraint stress and cosyntropin-stimulation testing on successive days) and necroscopy. Created in BioRender. Gaston, L. (2025) https://BioRender.com/sv70hla.

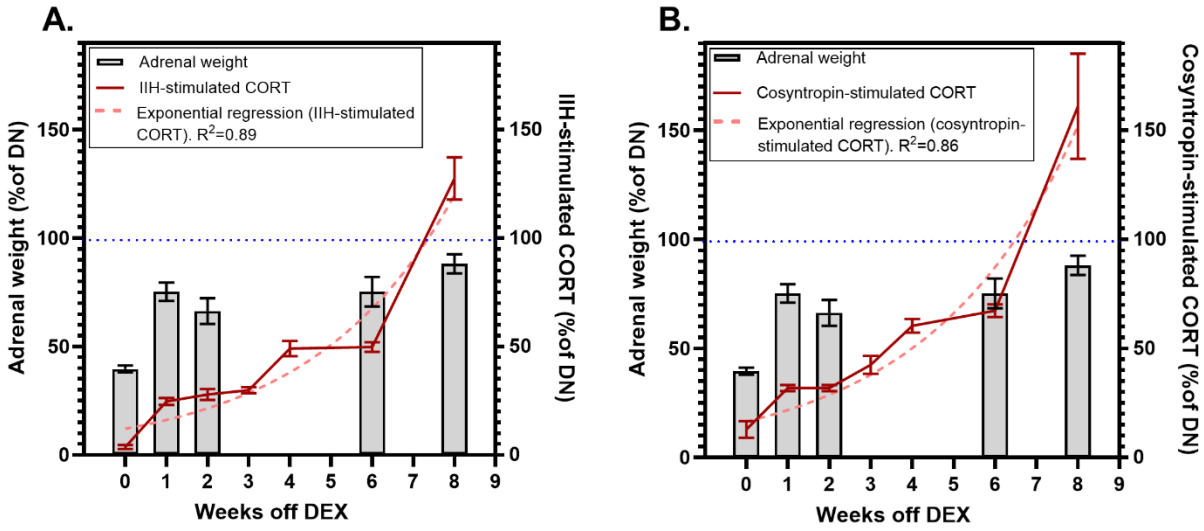

Fig. S2. Adrenal mass and stimulated CORT secretion follow different recovery trajectories after long-term DEX exposure. Adrenal weights (left Y-axis, gray bars) and A) insulin-induced hypoglycemia (IIH)-stimulated- or B) cosyntropin-stimulated CORT secretion (right Y-axis, red solid line) vs. weeks after withdrawal of 8 weeks of DEX treatment (X-axis). Adrenal weight data in A and B are identical and derived from those in Fig. 3A as a percentage of the Fig. 3A DN controls. CORT data are derived from those in Figs. 2F and 2G as a percentage of their DN controls. Pink dashed lines denote exponential growth models for IIH-stimulated ($Y = 12.1 * e^{0.29X}$, doubling time = 2.4 weeks, R^2=0.89) and cosyntropin-stimulated ($Y = 16.5 * e^{0.28X}$, doubling time = 2.5 weeks, R^2=0.86) CORT secretion.

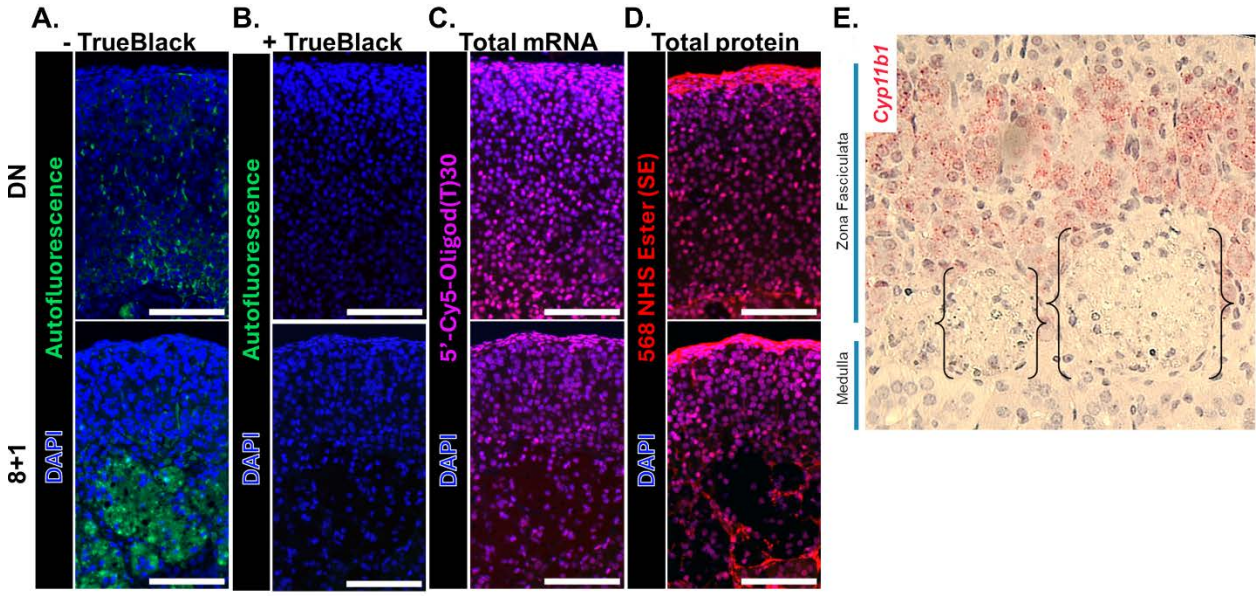

Fig. S3. The large, vacuolated structures that accumulate during long-term DEX treatment contain lipofuscin-rich, transcriptionally active cells rather than proteinaceous debris but are distinct from surrounding zona fasciculata cells. A) DEX-exposed adrenals (8+1, bottom) contain intensely autofluorescent clusters (green) that are absent in DN controls (top). B) Autofluorescence is eliminated with the addition of TrueBlack, a lipofuscin autofluorescence quencher. C) Nuclei within these clusters contain C) mature mRNA (*in situ* hybridization for total polyA with 5'-Cy5-Oligo d(T)30, magenta; with TrueBlack). D) The surrounding area is not intensely labeled by 568 NHS Ester (red; with TrueBlack), a total protein stain. All scale bars=100 microns (B-D). E) Cells in these clusters do not express the steroidogenic enzyme *Cyp11b1*, a zF marker (red, *in situ* hybridization using RNAScope with hematoxylin nuclear counterstain).

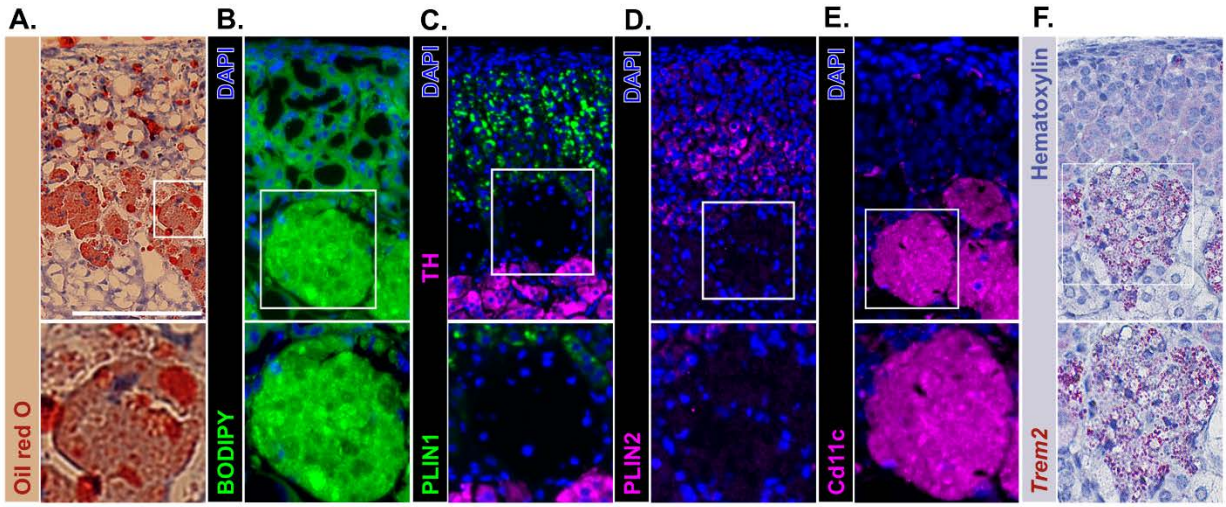

Fig. S4. Adrenal macrophages in DEX-exposed adrenals are lipid-laden, negative for lipid droplet associated proteins perilipin-1 and 2, and express some genes characteristic of lipid-associated macrophages. For all stains, representative images shown from 8+1 adrenals (top) with magnification of a macrophage cluster (bottom). A) Oil red O and B) BODIPY 493/503 staining. Immunofluorescence for C) perilipin-1 (PLIN1; green) with tyrosine hydroxylase (TH; magenta) to label the adrenal medulla, D) perilpin-2 (PLIN2; magenta), and E) Cd11c (magenta). F) *In situ hybridization* (RNAScope) for *Trem2* (red) with hematoxylin nuclear counterstain.

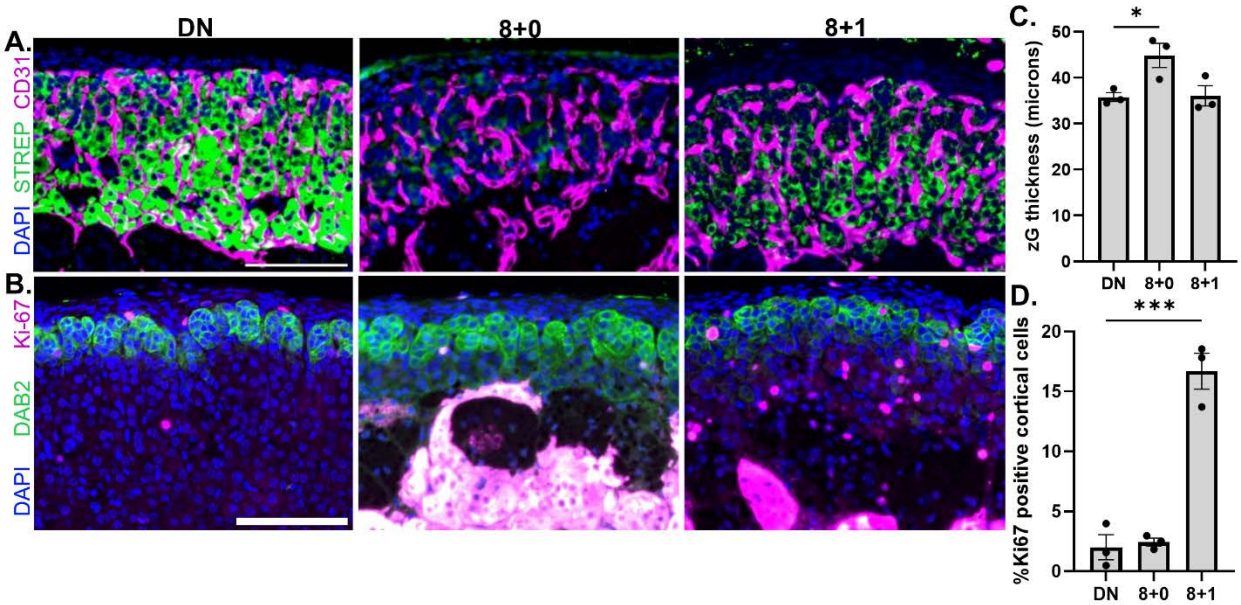

Fig. S5. DEX-withdrawn adrenals have an intact vascular network, normal zG thickness, and a marked increase in zF proliferation. Immunofluorescence for A) for the vascular marker CD31 (magenta) with a 488-streptavidin counterstain (green) to mark steroidogenic cortical cells and B) the proliferative marker Ki-67 (magenta) with Dab2 (green) to define the zG. Representative images from DN, 8+0, and 8+1 glands with quantification of C) zG thickness, and D) the percentage of Ki-67 positive adrenocortical cells. *$p<0.05$ and *** $p<0.001$ vs. DN.

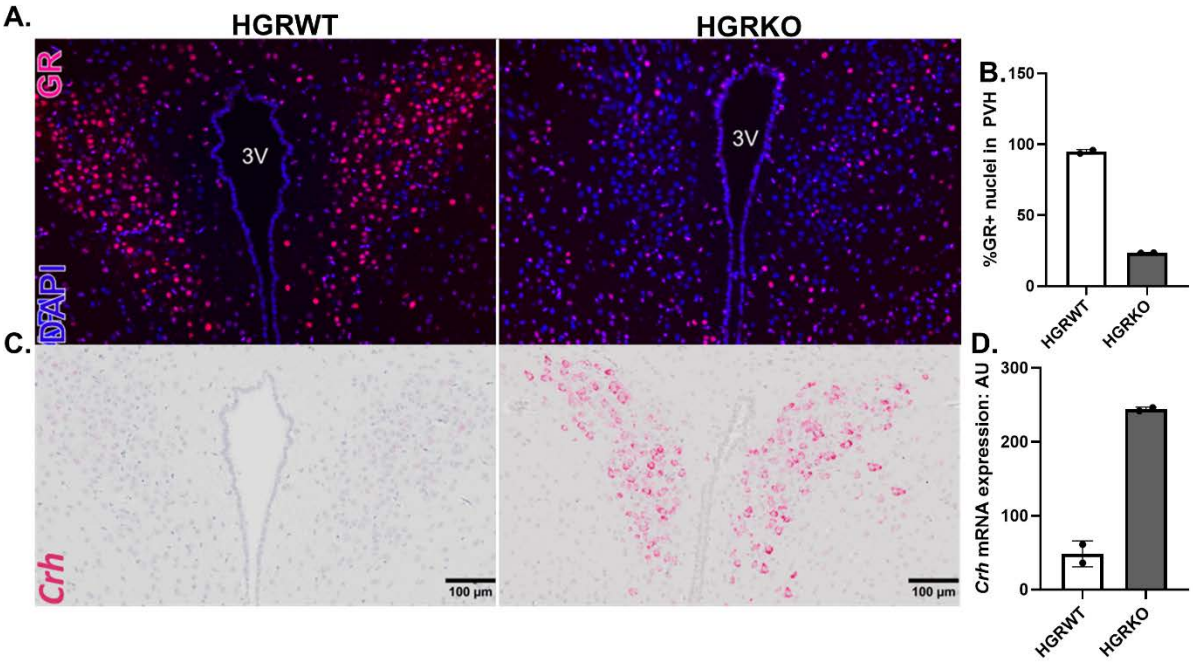

Fig. S6. Selective deletion of the glucocorticoid receptor from hypothalamic neurons protects against glucocorticoid-mediated suppression of *Crh* expression. A) Immunofluorescence for the glucocorticoid receptor (GR, red; DAPI, blue) in the paraventricular nucleus of the hypothalamus (PVH) of DEX-treated HGRWT (Cre-negative controls; left panel) and HGRKO (Sim1^{Cre+}:GR$^{fl/fl}$; right panel) mice with B) quantification of the percentage of GR-positive nuclei. C) *In situ* hybridization (RNAScope) for *Crh* (red) in PVH sections from DEX-treated HGRWT and HGRKO animals with D) quantification.

Table SI. PCR primers and settings for genotyping Sim1^{Cre}:GR$^{fl/fl}$ mice and controls (HGRKO and HGRWT).

Genotype reaction	Primer sequence	PCR settings
GR FLOX	Forward: ATG CCT GCT AGG CAA ATG AT Reverse: TTC CAG GGC TAT AGG AAG CA	Stage 1: 95 ℃ 3 min (1x); Stage 2: 95 ℃ 30 sec - 56 ℃ 30 sec - 52 ℃ 30 sec (10x); Stage 3: 68 ℃ 1 min (1x); Stage 4: 95 ℃ 30 sec - 53 ℃ 30 sec - 68 ℃ 2 min (35x); Stage 5: 68 ℃ 2 min (1x) 4℃ hold
Common Cre	Forward: TGC ATG ATC TCC GGT ATT GA Reverse: CGT ACT GAC GGT GGG AGA AT	Stage 1: 94 ℃ 2 min (1x); Stage 2: 94 ℃ 30 sec - 55 ℃ 30 sec - 72 ℃ 1 min (30x) Stage 3: 72 ℃ 5 min (1x) 4 ℃ hold

Table SII. Antibodies used for paraffin section immunofluorescence

Antibody	Antigen retrieval	Dilution	Company	Catalog number
Primary antibodies				
Rabbit anti-CD68	Sodium Citrate pH 6.0	1:750	abcam	ab125212
Rabbit anti-F4/80	Tris-EDTA pH 9.0	1:100	CST	70076T
Rabbit anti-Perilipin-1	Sodium Citrate pH 6.0	1:100	CST	9349
Rabbit anti-Perilipin-2	Tris-EDTA pH 9.0	1:200	CST	95109
Rabbit anti-Cd11c	Tris-EDTA pH 9.0	1:300	CST	97585
Sheep anti-tyrosine hydroxylase	Tris-EDTA pH 9.0	1:5000	Sigma Aldrich	AB1542
Rabbit anti-CD31	Tris-EDTA pH 9.0	1:100	CST	77699
Rabbit anti-Ki-67	Tris-EDTA pH 9.0	1:100	CST	D3B5
Mouse (IgG1) anti-Dab2	Tris-EDTA pH 9.0	1:200	BD Biosciences	610464
Secondary antibodies				
Donkey anti-rabbit IgG/647		1:200	Invitrogen	A-31573
Donkey anti-rabbit IgG/488		1:200	Invitrogen	A-21206
Goat anti-mouse IgG1/568		1:200	Invitrogen	A-21124
Donkey anti-sheep IgG		1:100	Invitrogen	A-21448